0026-895X/07/7204-812–825$20.00
MOLECULAR PHARMACOLOGY
Vol. 72, No. 4
38075/3250509
Printed in U.S.A.

Mol Pharmacol 72:812–825, 2007

Live Cell Analysis of G Protein β_5 Complex Formation, Function, and Targeting

Evan A. Yost, Stacy M. Mervine, Jonathan L. Sabo, Thomas R. Hynes, and Catherine H. Berlot

Weis Center for Research, Geisinger Clinic, Danville, Pennsylvania

Received May 11, 2007; accepted June 26, 2007

ABSTRACT

The G protein β_5 subunit differs from other β subunits in having divergent sequence and subcellular localization patterns. Although $\beta_5\gamma_2$ modulates effectors, β_5 associates with R7 family regulators of G protein signaling (RGS) proteins when purified from tissues. To investigate β_5 complex formation in vivo, we used multicolor bimolecular fluorescence complementation in human embryonic kidney 293 cells to compare the abilities of 7 γ subunits and RGS7 to compete for interaction with β_5. Among the γ subunits, β_5 interacted preferentially with γ_2, followed by γ_7, and efficacy of phospholipase C-β2 activation correlated with amount of $\beta_5\gamma$ complex formation. β_5 also slightly preferred γ_2 over RGS7. In the presence of coexpressed R7 family binding protein (R7BP), β_5 interacted similarly with γ_2 and RGS7. Moreover, γ_2 interacted preferentially with β_1 rather than β_5. These results suggest that multiple coexpressed proteins influence β_5 complex formation. Fluorescent $\beta_5\gamma_2$ labeled discrete intracellular structures including the endoplasmic reticulum and Golgi apparatus, whereas β_5RGS7 stained the cytoplasm diffusely. Coexpression of α_o targeted both β_5 complexes to the plasma membrane, and α_q also targeted $\beta_5\gamma_2$ to the plasma membrane. The constitutively activated α_o mutant, α_oR179C, produced greater targeting of β_5RGS7 and less of $\beta_5\gamma_2$ than did α_o. These results suggest that α_o may cycle between interactions with $\beta_5\gamma_2$ or other $\beta\gamma$ complexes when inactive, and β_5RGS7 when active. Moreover, the ability of $\beta_5\gamma_2$ to be targeted to the plasma membrane by α subunits suggests that functional $\beta_5\gamma_2$ complexes can form in intact cells and mediate signaling by G protein-coupled receptors.

In contrast to the other four members of the G protein β subunit family, which share 80% amino acid sequence identity, β_5 shares only 50% amino acid identity with these other β subunits and exhibits less association with cell membranes (Watson et al., 1994; Jones et al., 2004). Also, unlike the other β subunits, β_5 can associate with RGS proteins in the R7 family (RGS6, RGS7, RGS9, and RGS11), which interact with β_5 via their G protein γ-like (GGL) domain (Jones et al., 2004). β_5R7 complexes can activate the GTPase activity of α_o (Posner et al., 1999; Hooks et al., 2003) and accelerate both the activation and deactivation kinetics of GIRK channels (Kovoor et al., 2000; Drenan et al., 2006). Coexpression of β_5 and RGS7 increases the expression levels of both proteins compared with when they are expressed individually (Witherow et al., 2000), and mice lacking β_5 have reduced levels of R7 family RGS proteins (Chen et al., 2003), suggesting that these proteins are obligate dimers.

Whether β_5 also interacts with G protein γ subunits in vivo is controversial. $\beta_5\gamma_2$ can activate phospholipase C-β_2 (Watson et al., 1994; Zhang et al., 1996; Lindorfer et al., 1998) and inhibit GIRK channels (Mirshahi et al., 2002; Lei et al., 2003) and N-type Ca^{+2} channels (Zhou et al., 2000). However, when purified from native tissues, β_5 is associated with R7 family RGS proteins rather than γ subunits (Witherow et al., 2000). Complicating the issue, $\beta_5\gamma_2$ dimers are unstable under nondenaturing buffer conditions (Jones and Garrison, 1999; Jones et al., 2004), which could explain why they have yet to be isolated.

Because G protein-coupled receptors and G protein α subunits localize predominantly to the plasma membrane, complexes between β_5 and either R7 family proteins or γ subunits would be expected to localize there as well to modulate signaling. Plasma membrane targeting of β_5R7 complexes is promoted by association with both α_o (Takida et al., 2005) and R7BP (Drenan et al., 2006). Using BiFC, which involves

This work was supported by National Institutes of Health grant GM50369.
Article, publication date, and citation information can be found at http://molpharm.aspetjournals.org.
doi:10.1124/mol.107.038075.

ABBREVIATIONS: GGL, G protein γ-like; RGS, regulators of G protein signaling; BiFC, bimolecular fluorescence complementation; YFP, yellow fluorescent protein; CFP, cyan fluorescent protein; GFP, green fluorescent protein; ECFP, enhanced cyan fluorescent protein; HEK, human embryonic kidney; ER, endoplasmic reticulum; Cer, monomeric cerulean protein; R7BP, R7 family binding protein; 3D, three-dimensional; TIRF, total internal reflection fluorescence; GIRK, G protein-coupled inwardly rectifying potassium channel.

the reconstitution of a fluorescent signal from nonfluorescent fragments of YFP or CFP when they are fused to interacting proteins (Kerppola, 2006), we previously visualized complexes between β_5 and γ_1, γ_2, or γ_7 and found that they localized intracellularly rather than at the plasma membrane (Hynes et al., 2004b). This indicated that the β subunit could regulate targeting of $\beta\gamma$ complexes, because these same γ subunits localized to the plasma membrane when associated with other β subunits. The β subunit, unlike the γ subunit, is not known to contain modifications that cause membrane targeting (Wedegaertner et al., 1995). However, one means by which β subunits could regulate targeting would be via association with α subunits. Because α_o could target β_5RGS7 to the plasma membrane (Takida et al., 2005), we hypothesized that coexpression of α_o and/or other α subunits might lead to plasma membrane targeting of $\beta_5\gamma$ complexes.

Here, using live cell-based assays, we address the issues of which proteins β_5 forms complexes with, how complex formation and functionality are related, which α subunits β_5 complexes interact with, when in the GTPase cycle these interactions take place, and how the localization of β_5 complexes is regulated. Using multicolor BiFC, we compare the abilities of seven γ subunits (γ_1, γ_2, γ_5, γ_7, γ_{10}, γ_{11}, and γ_{12}) and RGS7 to compete for interaction with β_5. Using a plasma membrane targeting assay, we compare the abilities of active and inactive α_o to target $\beta_5\gamma_2$ and β_5RGS7 to the plasma membrane and of α_o and α_q to target $\beta_5\gamma_2$ to the plasma membrane. These studies demonstrate and quantify interactions that have not been detected using in vitro approaches and lead to a model for the roles of β_5 complexes in regulating G protein signaling.

Materials and Methods

Production of Fluorescent Fusion Protein and α Subunit Constructs. YFP-N-β_1 was produced as described previously (Hynes et al., 2004b). Cer-N-β_1 and Cer-N-β_5 were produced in the same manner as YFP-N-β_1 using the human β_1 and β_5 cDNAs and Cer(1–158)pcDNAI/Amp, which was produced as described previously (Mervine et al., 2006) using monomeric Cerulean (Rizzo et al., 2004) (obtained from David Piston, Vanderbilt University, Nashville, TN), which contains S72A, Y145A, H148D, and A206K substitutions in ECFP. Cer-N-RGS7 was produced in the same manner as Cer-N-β_1 and Cer-N-β_5 using human RGS7-S2 (Guthrie cDNA Resource Center, Sayre, PA). For CFP-N-RGS7t, the procedure was the same except that the sequence amino terminal to the GGL domain was deleted by amplifying RGS7 residues 202 to 479 and the polymerase chain reaction product was subcloned into CFP(1–158)pcDNAI/Amp. Cer-N-γ constructs and CFP-C-β_1 were produced as described previously (Mervine et al., 2006). YFP-N-γ_2 was produced in the same manner as the Cer-N-γ constructs, using YFP(1–158)pcDNAI/Amp (Hynes et al., 2004b). CFP-C-β_5 and CFP-C-γ_2 were produced in the same manner as CFP-C-β_1, using the human β_5 and γ_2 cDNAs, respectively. Cer-C-β_5 was produced in the same manner as CFP-C-β_5, using Cer(159–238)pcDNAI/Amp.

mCherry-Mem was produced as described for mRFP-Mem (Mervine et al., 2006) except that mCherry (Shaner et al., 2004) (obtained from Roger Tsien, University of California, San Diego, CA) was used as the polymerase chain reaction template. pEYFP-Golgi, encoding a fusion protein consisting of EYFP and the amino-terminal 81 residues of human beta1,4-galactosyltransferase, which targets to the trans-medial region of the Golgi apparatus, was obtained from Clontech (Mountain View, CA). pEYFP-ER, encoding a fusion protein consisting of EYFP with the ER targeting sequence of calreticulin at the amino terminal end and the ER retrieval sequence, KDEL, at the carboxyl terminal end, was obtained from Clontech. pGM130-EGFP, encoding a fusion protein consisting of EGFP and GM130, a *cis*-Golgi matrix protein, was obtained from Graham Warren (Yale University, New Haven, CT).

3FLAG-R7BP, consisting of the R7BP coding region subcloned into p3FLAG-CMV10 (Sigma-Aldrich, St. Louis, MO) was obtained from Kendall Blumer (Washington University, St. Louis, MO). The human phospholipase C-β2 cDNA in pRc/CMV (Invitrogen, Carlsbad, CA) was obtained from Ravi Iyengar (Mount Sinai School of Medicine, New York, NY).

The EE epitope (EYMPTE) was introduced into the rat $\alpha_{o\text{-}1}$ cDNA by replacing Asp167 with Glu and Gln169 with Met and Arg179 in α_o-EE was replaced by Cys to produce α_oR179C-EE by oligonucleotide-directed in vitro mutagenesis using the Bio-Rad Muta-Gene kit. α_s-YFP was produced as described for α_s-CFP (Hynes et al., 2004a) except that EYFP (Clontech) containing a substitution of Met for Gln69 was substituted for ECFP. α_q-YFPpcDNAI/Amp was produced from α_q-GFP/pcDNAI/Amp (Hughes et al., 2001). EYFP (Clontech) containing a substitution of Met for Gln69 and including *S*-G-G-G-G-S linkers on each end was substituted for GFP containing the same linkers as a BamHI/SacI cassette. This substitution was performed after the other BamHI and SacI sites in α_q-GFP were removed by silent mutations using oligonucleotide-directed in vitro mutagenesis and α_q-GFP was subcloned as a NotI insert into a modified version of pGEM-HE (Hughes et al., 2001) containing no BamHI or SacI sites. The resultant α_q-YFP cDNA was then subcloned into pcDNAI/Amp as a NotI insert. To produce α_o-YFP, a BglII site in the 5′ untranslated region of α_o-EE/pcDNAI/Amp was removed by digestion with T4 DNA polymerase and religation and then a unique BglII site was introduced in frame between Pro119 and Phe120 in the αB/αC loop of the helical domain, analogous to the YFP insertion site in α_q-YFP, using polymerase chain reactions that produced DNA fragments with overlapping ends that were combined subsequently in a fusion polymerase chain reaction. EYFP (Clontech, Moutain View, CA) containing a substitution of Met for Gln69 and including S-G-G-G-G-S linkers on each end was then subcloned into the BglII site as a BamHI cassette. All α subunit constructs used in this study contain the EE epitope. Henceforth in the text the EE designation is omitted for simplicity. All of the above constructs were verified by DNA sequencing.

Imaging of Transfected Cells by Spinning Disc Confocal Microscopy. HEK-293 cells (American Type Culture Collection, Manassas, VA) were plated at a density of 2×10^5 cells per well on four-well chambered coverslips (Lab-Tek II; Nalge Nunc International, Rochester, NY). On the following day, the cells were transiently transfected using 0.25 μl of LipofectAMINE 2000 Reagent (Invitrogen). Plasmids were transfected as described in the legends to Figs. 1, 5, 7, 9, and 10. A membrane marker (YFP-Mem or mCherry-Mem) was included in all transfections.

Cells were imaged 2 days after transfection using a white-light, spinning-disc confocal microscope composed of an Olympus IX81 inverted microscope, UIS2 60× 1.42 numerical aperture objective, IX2-DSU spinning disc system, 100-W mercury arc lamp, Hamamatsu C9100-02 electron multiplier camera, Ludl filter wheels, shutters, and xy stage, under the control of IPLab software (BD Biosciences, San Jose, CA). Excitation and emission filters for CFP (438/24, 483/32), YFP (504/12, 542/27), Red (589/15, 632/22), and a triple dichroic (FF444/521/608) were obtained from Semrock (Rochester, NY). One hour before imaging, the culture medium was replaced with 20 mM HEPES-buffered minimal essential medium with Earle's salts without bicarbonate. Cells were imaged at 25°C. For each condition, cells from at least three independent transfections were imaged.

The criteria for selecting cells for imaging were visible expression of all transfected fluorescent constructs, a clear section of plasma membrane border with adjacent region of cytoplasm, and a defined nucleus. The background intensity was determined by averaging the

intensity of a region of pixels outside the cell and was subtracted from each image. All image processing was performed using IPlab software.

Normalized Cytoplasmic Standard Deviation. The normalized cytoplasmic standard deviation is a measure of the variation in pixel intensities within the cytoplasmic area of the cell. Using a Cintiq pen-based display screen (Wacom, Vancouver, WA), a membrane border 6 pixels wide and centered on the plasma membrane was drawn around the cell using the image of the plasma membrane marker. A separate nuclear border was drawn just inside the nucleus excluding any intensity in the nuclear membrane. The standard deviation of the intensities of pixels inside the membrane border and outside the nuclear border was calculated and normalized by dividing by the average intensity of the cytoplasmic pixels to correct for differences in the intensities of fluorescent complexes.

Nuclear-to-Cytoplasmic Intensity Ratio. The nuclear-to-cytoplasmic intensity ratio is a measure of the distribution of the labeled protein between the nuclear and cytoplasmic compartments and was determined using the membrane and nuclear borders defined above. The nuclear intensity was calculated as the average intensity of pixels in the nucleus including the border. The cytoplasmic intensity was calculated as the average intensity of pixels inside the membrane border and outside the nuclear border. The ratio is the nuclear intensity divided by the cytoplasmic intensity.

Plasma Membrane Fraction. The plasma membrane fraction is a measurement of the distribution of a labeled protein between the plasma membrane and cytoplasm and the method of its determination has been described in detail previously (Mervine et al., 2006). In brief, the plasma membrane-to-cytoplasm intensity ratio of the protein of interest is compared with that of plasma membrane and cytoplasm markers. A value of 0 corresponds to a completely cytoplasmic distribution, and a value of 1 corresponds to a completely plasma membrane distribution.

Colocalization of $\beta_5\gamma_2$ with ER and Golgi Markers. To visualize colocalization of $\beta_5\gamma_2$ with the ER or Golgi apparatus, Cer-C-β_5Cer-N-γ_2 was coexpressed in HEK-293 cells with YFP-ER, YFP-trans-medial Golgi, or GFP-*cis*-Golgi markers as described in the legend to Fig. 2. 3D Z-stacks (16 slices, 0.6 μm/slice) of live cells were collected on a Leica TCS SP2 confocal microscope using 458 nm and 514 nm laser lines for excitation of CFP and YFP. 3D Z-sections were analyzed because the regions of a cell with clear ER or Golgi structures often occur at different levels of focus. The Z-sections displayed in Fig. 2 were selected to highlight the structure of the coexpressed marker. Two color laser TIRF images were collected on a Nikon TE200-E microscope equipped with Perfect Focus, TIRF-2 illuminator, and 440 nm and 514 nm laser lines for excitation of CFP and YFP. To insure image registration, a triple-pass dichroic (Z442/514/594; Chroma, Brattleboro, VT) was used with emission filters in a motorized filter wheel (Ludl, Hawthorne, NY). The TIRF micrometer was motorized to control the TIRF angle for each laser line. Data collection was automated using IPLab software.

To visualize colocalization with each marker, a percentage of the 3D image of the ER or Golgi marker was subtracted from the $\beta_5\gamma_2$ image to generate a 3D subtracted image illustrating the remaining protein distribution that was not associated with the marker. The percentage subtracted was the amount that minimized the standard deviation of pixel intensities in the subtracted image, in the cytoplasm excluding the Golgi region for the ER marker, and in the cytoplasm region that included the Golgi region for the Golgi marker. The standard deviation minimum indicated that pixel intensity variations resulting from visible ER or Golgi structures had been optimally subtracted.

Measurement of Fluorescence in Cell Populations. HEK-293 cells (1.6×10^6 per 60-mm dish) were transfected with plasmids as described in the legends to Figs. 3, 4, 6, 7, and 8 using 6 μl of Lipofectamine 2000 Reagent (Invitrogen) according to the manufacturer's instructions. Two days later, cells were washed once in 4 ml of HBSS + $CaCl_2$ media (20 mM HEPES, pH 7.2, 118 mM NaCl, 4.6 mM KCl, 10 mM D-glucose, and 1 mM $CaCl_2$). Two milliliters of HBSS + EDTA media (20 mM HEPES, pH 7.2, 118 mM NaCl, 4.6 mM KCl, 10 mM D-glucose, and 0.5 mM EDTA) were then added to the dish, and the cells were scraped off with a rubber policeman and resuspended in a 1-cm square glass cuvette with a magnetic stir bar.

Data were collected on a PC1 photon-counting spectrofluorometer (ISS, Champaign, IL) configured with motorized filter wheels on both the excitation path between the excitation monochrometer and the sample, and on the emission path between the sample and the emission monochrometer as described previously (Mervine et al., 2006).

In multicolor BiFC experiments, the IC_{50} for inhibition of association of YFP-N-γ_2 with CFP-C-β_5 by Cer-N-γ subunits or Cer-N-RGS7 was defined as micrograms of Cer-N-γ subunit or Cer-N-RGS7 plasmid that produced a 50% decrease in the intensity of CFP-C-β_5YFP-N-γ_2. To determine IC_{50} values, the data were fit, using Kaleidograph (Abelbeck/Synergy Software, Reading, PA), to $Y = (100)/(1 + (X/a)^b)$, where X is micrograms of of transfected Cer-N-γ or Cer-N-RGS7 plasmid, Y is the percentage of maximal fluorescence produced by CFP-C-β_5YFP-N-γ_2, a is the half-maximal inhibitory concentration (IC_{50}) of the Cer-N-γ subunit or Cer-N-RGS7, and b is the slope factor. The IC_{50} for inhibition of association of YFP-N-β_1 with CFP-C-γ_2 by Cer-N-β subunits was determined in the same manner.

Immunoblots. The expression levels of Cer-N-proteins were determined in HEK-293 cells (1.6×10^6 per 60-mm dish) that were transfected as described in the legends to Figs. 3, 6, 7, and 8 using 6 μl of Lipofectamine 2000 Reagent. Two days after transfection, total cell lysates (7.5 or 15 μg) were resolved on NuPAGE Bis-Tris 4 to 12% gels (Invitrogen) and transferred to nitrocellulose. The expression levels of the Cer-N-γ subunits were determined for Fig. 3 by probing with a polyclonal antibody to residues 3 to 17 of GFP (Anti-GFP, N-terminal; Sigma-Aldrich, St. Louis, MO), and the expression levels of Cer-N-γ_2 and Cer-N-RGS7 were determined for Figs. 6 and 7 by probing with a polyclonal antibody to full-length GFP (Rockland Immunochemicals, Gilbertsville, PA). The antigen-antibody complexes were detected according to the ECL Western blotting protocol (GE Healthcare, Chalfont St. Giles, Buckinghamshire, UK). Chemiluminescence was imaged using a Lumi-Imager (Roche Applied Science, Indianapolis, IN). The expression levels of Cer-N-β_1 and Cer-N-β_5 were determined for Fig. 8 by probing with a polyclonal antibody to full-length GFP (Rockland Immunochemicals). The antigen-antibody complexes were detected using SuperSignal West Pico Chemiluminescent Substrate (Pierce Biotechnology, Rockford, IL). Chemiluminescence was imaged using a FluorChem SP Imaging System (Alpha Innotech, San Leandro, California). Bands in the images were quantified using IPLab software.

The expression levels of EE-tagged α subunits were determined for Fig. 9 using membranes prepared as described previously (Medina et al., 1996) 2 days after transfection of HEK-293 cells (4.45×10^6/100-mm dish) with 4.45 μg of each α subunit plasmid using 5.56 μl of LipofectAMINE 2000 Reagent. 50 μg of membrane proteins were resolved by SDS-polyacrylamide electrophoresis (10%), transferred to nitrocellulose, and probed with a monoclonal antibody to the EE epitope. The antigen-antibody complexes were detected according to the ECL Western blotting protocol and chemiluminescence was imaged using a Lumi-Imager. Bands in the images were quantified using IPLab software.

Assay for Inositol Phosphate Accumulation in Transiently Transfected Cells. HEK-293 cells (1.6×10^6 per 60-mm dish) were transfected with plasmids as described in the legend to Fig. 4 using 6 μl of Lipofectamine 2000 Reagent according to the manufacturer's instructions. Twenty-four hours after transfection, the cells were replated in 24-well plates and labeled with [^{3}H]inositol (GE Healthcare). After an additional 24 h, inositol phosphate levels were determined in the presence of 5 mM LiCl as described previously (Medina et al., 1996).

Results

Complexes of β_5 with Different γ Subunits Exhibited Distinct Localization Patterns. We investigated the ability of β_5 to form complexes with γ_1, γ_2, γ_5, γ_7, γ_{10}, γ_{11}, and γ_{12} in HEK-293 cells. β_5 (Wang et al., 1999a) and each of these γ subunits, with the exception of γ_1 (Wang et al., 1997), have been detected at the protein level in these cells. $\beta_5\gamma$ complexes were imaged using BiFC, which involves the production of fluorescence by two nonfluorescent fragments of CFP or YFP when they are brought together by interactions between proteins fused to each fragment. In contrast to fluorescence resonance energy transfer (FRET), in which the intensity of the signal depends on the distance between and relative orientation of two fluorophores, BiFC is based on the formation of a fluorescent complex from nonfluorescent constituents and does not require that the interacting proteins position the fluorescent protein fragments in a specific orientation or within a fixed distance from each other (Kerppola, 2006). However, steric constraints can prevent the association of the fluorescent protein fragments within a complex, in which case inserting peptide linkers between the fragments and the interacting proteins may enable association of the fluorescent fragments (Kerppola, 2006). We applied the BiFC approach previously to image $\beta_1\gamma$ complexes, which were demonstrated to be functional by their abilities to potentiate activation of adenylyl cyclase by α_s in COS-7 cells (Hynes et al., 2004b) and to internalize in response to stimulation of the β_2-adrenergic receptor in HEK-293 cells (Hynes et al., 2004a). For live cell imaging, we fused a carboxyl-terminal fragment (residues 159–238) of cerulean, an engineered form of ECFP that is 2.5-fold brighter than ECFP (Rizzo et al., 2004), to β_5 to produce Cer-C-β_5, and an amino-terminal cerulean fragment (residues 1–158) to the γ subunits, producing Cer-N-γ subunits.

Each of the Cer-C-β_5Cer-N-γ complexes produced a fluorescent signal (Fig. 1, A–G). However, Cer-C-β_5 and Cer-N-γ_2, which produced one of the brightest signals when coexpressed, were not fluorescent when expressed individually (data not shown). The localization patterns of the $\beta_5\gamma$ complexes varied depending on the associated γ subunit (Fig. 1), in agreement with a previous study of a subset of these $\beta_5\gamma$ complexes (Hynes et al., 2004b), and in contrast to the corresponding $\beta_1\gamma$ complexes, which localized predominantly to the plasma membrane (Mervine et al., 2006). The $\beta_5\gamma$ complexes exhibited very little plasma membrane signal and varied in their distribution between the cytoplasm and the nucleus (Fig. 1, A–G, and J). $\beta_5\gamma_1$, $\beta_5\gamma_5$, $\beta_5\gamma_{10}$, and $\beta_5\gamma_{11}$ exhibited relatively high ratios of nuclear to cytoplasmic signal (0.63–0.88) (Fig. 1A, C, E, F, and J), whereas $\beta_5\gamma_2$, $\beta_5\gamma_7$, and $\beta_5\gamma_{12}$ exhibited lower ratios of nuclear-to-cytoplasmic signal (0.36–0.45) (Fig. 1B, D, G, and J). For comparison, α_s, which, when over-expressed without exogenous $\beta\gamma$, labels the cytoplasm diffusely (Mervine et al., 2006) (Fig. 1H), yielded a ratio of nuclear-to-cytoplasmic signal (0.34) similar to that of $\beta_5\gamma_2$ and $\beta_5\gamma_7$ (Fig. 1J), suggesting that this amount of nuclear signal represents background labeling by proteins that are excluded from the nucleus. In contrast, mCherry, which diffuses freely between the nucleus and cytoplasm (Fig. 1I), exhibited a nuclear-to-cytoplasmic signal ratio of 0.97 (Fig. 1J).

The $\beta_5\gamma$ complexes also varied in the degree to which their cytoplasmic signals were diffuse or associated with discrete intracellular structures (Fig. 1, A–G). This aspect of the cytoplasmic $\beta_5\gamma$ signals was quantified by determining normalized cytoplasmic standard deviations of pixel intensity as described under *Materials and Methods*. This measurement indicates the extent to which labeled proteins in the cytoplasm are distributed evenly as free soluble proteins (low

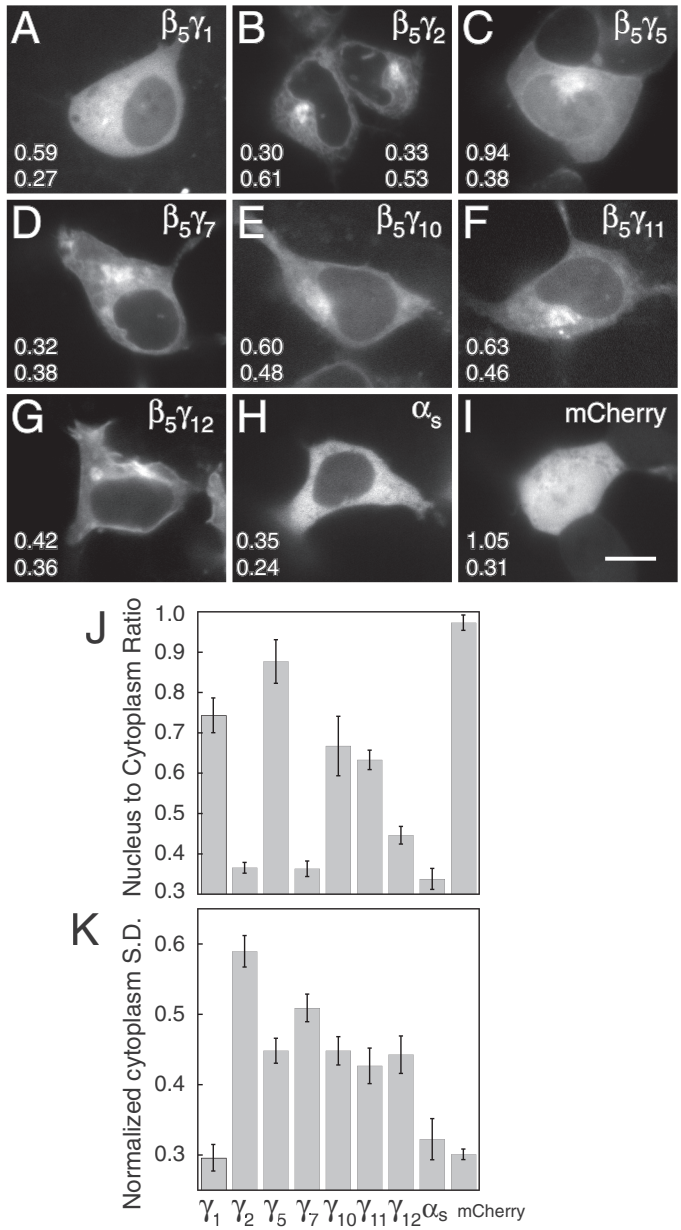

Fig. 1. Complexes of β_5 with γ_1, γ_2, γ_5, γ_7, γ_{10}, γ_{11}, and γ_{12} exhibit distinct localization patterns. A–I, images of HEK-293 cells expressing the indicated Cer-C-β_5Cer-N-γ complexes (A–G), α_s-YFP (H), or mCherry (I). HEK-293 cells were transfected with the following quantities of plasmids: Cer-C-β_5, 0.075 μg; Cer-N-γ subunits, 0.075 μg; YFP-Mem, 0.0025 μg; mCherry, 0.0125 μg (A–G); α_s-YFP, 0.15 μg; mCherry-Mem, 0.0025 μg (H); and mCherry, 0.0125 μg (I). The top numbers in the images are the ratios of average pixel intensity in the nucleus to that in the cytoplasm and the bottom numbers are the normalized cytoplasmic standard deviations of pixel intensity for the cells shown. J, ratios of average pixel intensity in the nucleus compared with the cytoplasm. K, normalized cytoplasmic standard deviations of pixel intensity for the indicated constructs. Values represent the means ± S.E. The numbers of cells analyzed are as follows: $\beta_5\gamma_1$, 39; $\beta_5\gamma_2$, 62; $\beta_5\gamma_5$, 45; $\beta_5\gamma_7$, 54; $\beta_5\gamma_{10}$, 44; $\beta_5\gamma_{11}$, 41; $\beta_5\gamma_{12}$, 50; α_s, 19; and mCherry, 335. Scale bar, 10 μm.

standard deviation), as opposed to being localized on discrete vesicles, membranes, or other structures that would increase the range of pixel intensities significantly (high standard deviation). Lower standard deviations were associated with the diffuse labeling patterns of α_s-YFP and mCherry (Fig. 1, H, I, and K). This analysis showed that $\beta_5\gamma_1$ exhibited by far the lowest standard deviation and was comparable with α_s-YFP and mCherry (Fig. 1K). In contrast, $\beta_5\gamma_2$ and $\beta_5\gamma_7$ had the greatest standard deviation. The other $\beta_5\gamma$ complexes had values that were closer to those of $\beta_5\gamma_2$ and $\beta_5\gamma_7$ than to that of $\beta_5\gamma_1$. The diffuse nature of the $\beta_5\gamma_1$ signal may be due, in part, to the fact that γ_1 is farnesylated, rather than geranylgeranylated (Wedegaertner et al., 1995). However, because γ_{11} is also farnesylated and $\beta_5\gamma_{11}$ exhibited much more discrete staining than did $\beta_5\gamma_1$, additional differences between γ_1 and the other γ subunits seem to be important in determining the nature of the signal. In summary, these results show that the partitioning of $\beta_5\gamma$ complexes between the cytoplasm and the nucleus and the nature of their distribution in the cytoplasm (diffuse or discrete) are determined by the γ subunit component.

The discrete cytoplasmic labeling observed with some of the $\beta_5\gamma$ complexes, notably $\beta_5\gamma_2$, seemed to reside on a number of intracellular structures, primarily the ER, Golgi apparatus, and nuclear membrane. To define the localization of these complexes more precisely, 3D stacks of images of $\beta_5\gamma_2$ coexpressed with markers for the ER or the Golgi apparatus were collected on a laser-scanning confocal microscope (Fig. 2, A and C). Colocalization of $\beta_5\gamma_2$ with both the ER and trans-medial Golgi apparatus was observed in the merge images (Fig. 2, A and C). Colocalization with a *cis*-Golgi marker was similar to that seen with the trans-medial Golgi marker (data not shown). To visualize $\beta_5\gamma_2$ distribution not associated with the coexpressed markers, the marker images were subtracted from the $\beta_5\gamma_2$ images as described under *Materials and Methods*. After subtraction of the ER images from the $\beta_5\gamma_2$ images, significant intensity remained in the perinuclear region, as well as some diffuse cytoplasmic and nuclear membrane intensity (Fig. 2A). The perinuclear intensity of $\beta_5\gamma_2$ was due primarily to the Golgi apparatus, with clear colocalization in the merge image and very little signal visible above the surrounding intensity of the ER and diffuse cytoplasm staining in the subtracted image (Fig. 2C). Colocalization of $\beta_5\gamma_2$ with the ER marker was also observed using a two-color laser TIRF microscope, where the densely packed folds of the ER membranes seen in the confocal cross-sections were visualized distinctly (Fig. 2B).

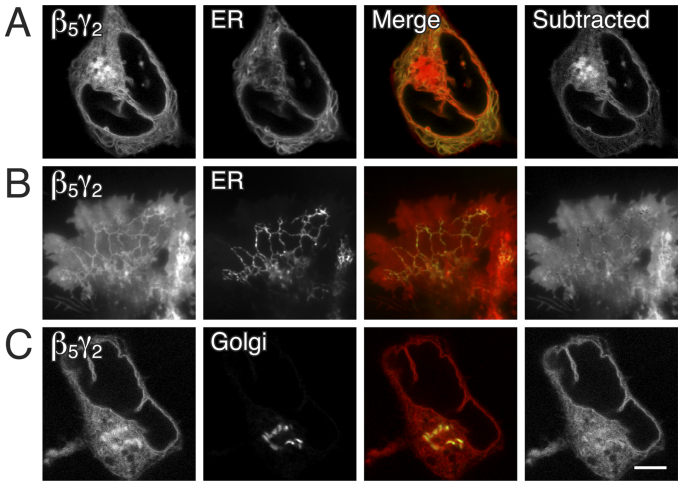

Fig. 2. $\beta_5\gamma_2$ exhibits colocalization with the ER and the Golgi complex. HEK-293 cells were transfected with the following quantities of plasmids: Cer-C-β_5, 0.075 μg; Cer-N-γ_2, 0.075 μg; either YFP-ER marker, 0.0025 μg (A and B) or YFP-trans-medial Golgi marker, 0.0025 μg (C); mCherry, 0.0125 μg. Cells were imaged using a Leica TCS SP2 confocal microscope (A and C) or a two-color laser TIRF microscope (B). Cer-C-β_5Cer-N-γ_2 complexes (first column of images) were simultaneously imaged with YFP-ER or YFP-Golgi markers in the same cell (second column of images). The third column is a merge of each set of images and demonstrates colocalization (yellow) of Cer-C-β_5Cer-N-γ_2 (red) with the YFP markers (green). Images in the fourth column were produced by subtracting a percentage of the YFP-ER or YFP-Golgi marker image from the corresponding Cer-C-β_5Cer-N-γ image as described under *Materials and Methods*. These images demonstrate that a substantial amount of the intracellular Cer-C-β_5Cer-N-γ_2 signal can be accounted for by either the ER or the Golgi apparatus. Scale bar, 10 μm. Images are representative of 10 cells (A), 16 cells (B), and 8 cells (C).

β_5 Interacted Preferentially with γ_2 Compared with γ_1, γ_5, γ_7, γ_{10}, γ_{11}, and γ_{12}. The intensities of CFP-C-β_5Cer-N-γ complexes were quantified in HEK-293 cell populations using a spectrofluorometer. In the presence of an excess of CFP-C-β_5, the intensities of the CFP-C-β_5Cer-N-γ complexes varied over a 100-fold range, with CFP-C-β_5Cer-N-γ_2 and CFP-C-β_5Cer-N-γ_1 being the most and least intense, respectively (Fig. 3A). This range was much greater than the 3-fold range seen previously when the intensities of the corresponding CFP-C-β_1Cer-N-γ complexes were compared under the same conditions (Mervine et al., 2006). The expression levels of the Cer-N-γ subunits, when coexpressed with excess CFP-C-β_5, were compared by immunoblotting total cell lysates with an antibody to the amino terminus of GFP (Fig. 3B). There was a larger range in expression levels than when the same Cer-N-γ subunits were coexpressed with an excess of CFP-C-β_1 (Mervine et al., 2006), suggesting that β_1 and β_5 differ in their abilities to stabilize these γ subunits. However, the range in Cer-N-γ expression levels (Fig. 3B) was narrower than the range in intensities of the CFP-C-β_5Cer-N-γ complexes (Fig. 3A). CFP-C-β_5Cer-N-γ_2 exhibited by far the highest ratio of CFP-C-β_5Cer-N-γ intensity to Cer-N-γ expression level, followed by CFP-C-β_5Cer-N-γ_7 (Fig. 3C). The CFP-C-β_5Cer-N-γ intensity-to-Cer-N-γ expression ratio of CFP-C-β_5Cer-N-γ_2 was 18.6-fold greater than that of CFP-C-β_5Cer-N-γ_{11}, which had the lowest ratio (Fig. 3C). In contrast, the intensity-to-Cer-N-γ expression ratios of the corresponding CFP-C-β_1Cer-N-γ complexes varied by 2-fold or less (Mervine et al., 2006).

Given that cells coexpress multiple isoforms of β and γ subunits, the predominance of particular $\beta\gamma$ complexes will be influenced both by the relative expression levels and the association preferences of the expressed β and γ subunits. Although CFP-C-β_5Cer-N-γ_2 was clearly the most intense complex when CFP-C-β_5 was not limiting, we sought to determine whether this was also the preferred complex when different γ subunits were coexpressed with a limiting amount of β_5 and whether differences between the less preferred γ subunits would be revealed under these conditions. Multicolor BiFC makes it possible to simultaneously image multiple complexes and quantify the abilities of different proteins to compete for a limiting amount of a common binding partner, because the amino terminal fragment of the fluorescent protein determines the spectral properties of the complex (Grinberg et al., 2004). We found previously that the intensities of CFP-C-β_1Cer-N-γ complexes were similar when

CFP-C-β_1 was not limiting, but when the intensities of coexpressed CFP-C-β_1Cer-N-γ (cyan) and CFP-C-β_1YFP-N-γ_2 (yellow) complexes were compared under conditions in which CFP-C-β_1 was limiting, the Cer-N-γ subunits exhibited an approximately 4.5-fold range in their abilities to compete with YFP-N-γ_2 for association with CFP-C-β_1 (Mervine et al., 2006).

The abilities of the Cer-N-γ subunits to compete with YFP-N-γ_2 for association with limiting amounts of CFP-C-β_5 were compared by determining the amounts of each Cer-N-γ subunit that decreased the intensity of CFP-C-β_5YFP-N-γ_2 by 50%. Cer-N-γ_2 competed 18-fold more effectively than Cer-N-γ_{10} (the least effective competitor) and 2.7-fold more effectively than the next best competitor, Cer-N-γ_7 (Fig. 3D, Table 1). When the amounts of transfected Cer-N-γ plasmids were normalized to their relative expression levels in the presence of limiting amounts of CFP-C-β_5, Cer-N-γ_2 was still the most effective Cer-N-γ subunit, competing 23-fold more effectively than Cer-N-γ_{11}, the least effective subunit (Fig. 3E, Table 1). When expression levels were corrected for, Cer-N-γ_1 became almost as effective in competition as Cer-N-γ_7. Cer-N-γ_2 was 4-fold more effective than Cer-N-γ_7 and 6.5-fold more effective than Cer-N-γ_1(Fig. 3E, Table 1). This range in the abilities of the Cer-N-γ subunits to compete for limiting amounts of CFP-C-β_5 was much greater than that of their abilities to compete for CFP-C-β_1 (Mervine et al., 2006) and the relative efficacies of the Cer-N-γ subunits were different, as described under *Discussion*.

Efficacy of Phospholipase C-β2 Activation by $\beta_5\gamma$ Combinations Was Correlated with the Amount of Complex Formation. Previous comparisons of the abilities of $\beta_5\gamma$ complexes to modulate effectors demonstrated that cells expressing $\beta_5\gamma_2$ exhibited greater phospholipase C-β2 activity than did cells expressing $\beta_5\gamma_1$, $\beta_5\gamma_3$, $\beta_5\gamma_4$, $\beta_5\gamma_5$, or $\beta_5\gamma_7$ (Watson et al., 1994; Watson et al., 1996) and N-type Ca^{+2} channel inhibition was obtained in cells expressing $\beta_5\gamma_2$ but not $\beta_5\gamma_1$ or $\beta_5\gamma_3$ (Zhou et al., 2000). These results indicated either that $\beta_5\gamma_2$ was more effective than the other $\beta_5\gamma$ complexes at modulating these effectors or that $\beta_5\gamma_2$ complexes formed preferentially relative to the other $\beta_5\gamma$ combinations. To distinguish between these two alternatives, we compared phospholipase C-β2 activity in cells expressing CFP-C-β_5 and different Cer-N-γ subunits with the relative amounts of CFP-C-β_5Cer-N-γ complex formation detected as

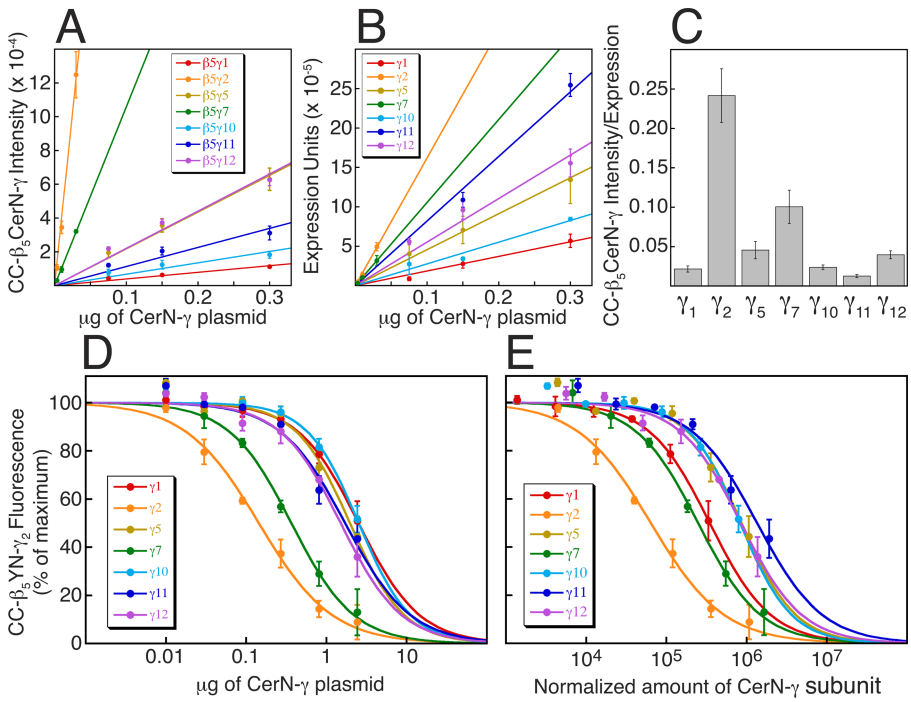

Fig. 3. β_5 interacts preferentially with γ_2 rather than γ_1, γ_5, γ_7, γ_{10}, γ_{11}, or γ_{12}. A, fluorescence intensities of CFP-C-β_5Cer-N-γ complexes when CFP-C-β_5 is not limiting. HEK-293 cells were transfected with 2.4 μg of plasmid expressing CFP-C-β_5 and the indicated μg of Cer-N-γ plasmids. The total amount of plasmid in each transfection was maintained at 2.7 μg by making up the difference with pcDNAI/Amp. Values represent the means ± S.E. from three experiments performed in duplicate. CFP-C-β_5Cer-N-γ intensities per microgram of Cer-N-γ plasmid, determined from linear fits to the data were as follows (means ± S.E, × 10^{-4}): $\beta_5\gamma_1$, 3.93 ± 0.27; $\beta_5\gamma_2$, 408 ± 44.8; $\beta_5\gamma_5$, 21.8 ± 2.36; $\beta_5\gamma_7$, 106 ± 4.34; $\beta_5\gamma_{10}$, 6.72 ± 0.94; $\beta_5\gamma_{11}$, 11.3 ± 1.40; and $\beta_5\gamma_{12}$, 22.0 ± 0.93. B, expression levels of Cer-N-γ subunits when coexpressed with an excess of CFP-C-β_5. HEK-293 cells were transfected as in A. Values represent the means ± S.E from three experiments. Cer-N-γ expression per microgram of plasmid, determined from linear fits to the data were as follows (means ± S.E, × 10^{-6}): γ_1, 1.82 ± 0.29; γ_2, 16.87 ± 1.50; γ_5, 4.77 ± 1.00; γ_7, 10.51 ± 2.13; γ_{10}, 2.78 ± 0.05; γ_{11}, 8.48 ± 0.28; and γ_{12}, 5.54 ± 0.59. C, normalization of CFP-C-β_5Cer-N-γ intensities to Cer-N-γ expression levels. The intensity per microgram of Cer-N-γ plasmid of each CFP-C-β_5Cer-N-γ complex was divided by the corresponding Cer-N-γ expression per microgram of plasmid. D, competition between Cer-N-γ subunits and YFP-N-γ_2 for limiting amounts of CFP-C-β_5. The intensity of CFP-C-β_5YFP-N-γ_2 was measured in the presence of each Cer-N-γ subunit or empty vector. HEK-293 cells were transfected with 0.6 μg each of plasmids expressing CFP-C-β_5 and YFP-N-γ_2, and the indicated micrograms of each Cer-N-γ plasmid. The total amount of plasmid in each transfection was maintained at 3.63 μg using pcDNAI/Amp. Values represent the means ± S.E. from three experiments performed in duplicate. E, CFP-C-β_5YFP-N-γ_2 intensity is expressed as a function of the relative amounts of coexpressed Cer-N-γ. Expression levels were determined in HEK-293 cells transfected with 0.6 μg each of plasmids expressing CFP-C-β_5 and pcDNAI/Amp, and 0.03, 0.09, 0.27, or 2.43 μg of each Cer-N-γ plasmid. The total amount of plasmid in each transfection was maintained at 3.63 μg using pcDNAI/Amp. The expression levels of the Cer-N-γ subunits varied linearly and the data were fit by linear regressions. The plasmid amounts used in D were multiplied by Cer-N-γ expression per microgram of plasmid to yield the normalized amount of each Cer-N-γ subunit. CC indicates CFP-C and YN indicates YFP-N.

BiFC. Four of the CFP-C-β_5Cer-N-γ complexes (those containing Cer-N-γ_2, Cer-N-γ_5, Cer-N-γ_7, or Cer-N-γ_{12}) activated coexpressed phospholipase C-β2, whereas the other three complexes (those containing Cer-N-γ_1, Cer-N-γ_{10}, or Cer-N-γ_{11}) produced no activation above that seen in cells transfected with empty vector (Fig. 4A). CFP-C-β_5Cer-N-γ_2 and CFP-C-β_5Cer-N-γ_7 exhibited the greatest activity. No activity was obtained when CFP-C-β_5 was expressed without a Cer-N-γ subunit or when any of the Cer-N-γ subunits was expressed without CFP-C-β_5 (Fig. 4A). The three CFP-C-β_5Cer-N-γ complexes that did not stimulate phospholipase C-β2 exhibited only minimal fluorescence, indicating that lack of activity was due to ineffective complex formation (Fig. 4B). For the 4 CFP-C-β_5Cer-N-γ complexes that activated phospholipase C-β2, the ratios of CFP-C-β_5Cer-N-γ-stimulated activity (Fig. 4A) to amount of complex formation (Fig. 4B) were similar (Fig. 4C), indicating that the different efficacies of the CFP-C-β_5Cer-N-γ combinations were due primarily to different amounts of complex formation. This is the first time that $\beta\gamma$ function in intact cells has been correlated directly with the amount of $\beta\gamma$ complex formation.

$\beta_5\gamma_2$ and β_5RGS7 Complexes in the Same Cell Could Be Imaged Simultaneously using BiFC. The above studies demonstrated that β_5 associates preferentially with γ_2 compared with the other γ subunits tested. To determine the association preference of β_5 for γ subunits versus R7 family RGS proteins and to compare the localization patterns of these β_5 complexes, we expressed fluorescent $\beta_5\gamma_2$ and β_5RGS7 complexes in the same cells. CFP-C-β_5 was coexpressed with Cer-N-RGS7 and YFP-N-γ_2 to produce CFP-C-β_5Cer-N-RGS7 (cyan) and CFP-C-β_5YFP-N-γ_2 (yellow). Both complexes exhibited minimal localization to the nucleus (Fig. 5, A–C and E), compared with $\beta_5\gamma_1$, $\beta_5\gamma_5$, $\beta_5\gamma_{10}$, and $\beta_5\gamma_{11}$ (Fig. 1J). However, CFP-C-β_5Cer-N-RGS7t, containing a truncated form of RGS7 in which the DEP domain was deleted, localized preferentially in the nucleus (Fig. 5, D and E), in agreement with a previous study of RGS6 splice variants that demonstrated that the DEP domain can function as a cytoplasmic retention signal (Chatterjee et al., 2003). In contrast to the distribution of CFP-C-β_5YFP-N-γ_2 on discrete structures in the cytoplasm (Fig. 5, A and C), the cytoplasmic signals of CFP-C-β_5Cer-N-RGS7 and CFP-C-β_5Cer-N-RGS7t were diffuse (Fig. 5, B and D). The different types of cytoplasmic signals were confirmed and quantified by the higher normalized standard deviation of cytoplasmic pixel intensity of CFP-C-β_5YFP-N-γ_2 compared with CFP-C-β_5Cer-N-RGS7 and CFP-C-β_5Cer-N-RGS7t (Fig. 5F). These results indicate that both γ subunits and R7 family RGS proteins can dictate the localization pattern of β_5. Fluorescence was not obtained when CFP-C-β_5, Cer-N-RGS7, or YFP-γ_2 were expressed alone (data not shown), and minimal fluorescence was obtained when CFP-C-β_1 and Cer-N-RGS7 were coexpressed (Fig. 6D), consistent with previous reports that β_1 and R7 family RGS proteins do not interact (Snow et al., 1998; Posner et al., 1999).

$\beta_5\gamma_2$ and β_5RGS7 Complexes Formed with Equal Efficiency When Excess β_5 Was Coexpressed with Either γ_2 or RGS7. In the presence of excess cotransfected CFP-C-β_5 plasmid, linear relationships between the amounts of transfected Cer-N-γ_2 and Cer-N-RGS7 plasmids and the intensities of CFP-C-β_5Cer-N-γ_2 and CFP-C-β_5Cer-N-RGS7 complexes, respectively, were obtained (Fig. 6A). The intensity of CFP-C-β_5Cer-N-γ_2 was 19-fold greater than that of CFP-C-β_5Cer-N-RGS7, based on the slopes of linear fits to the data. To determine whether this difference was due to a greater ability of CFP-C-β_5 to form fluorescent complexes with Cer-N-γ_2 compared with Cer-N-RGS7 or to differences in expression of the Cer-N fusion proteins, the expression levels of Cer-N-γ_2 and Cer-N-RGS7, when coexpressed with excess CFP-C-β_5, were determined using immunoblots. The slope of the linear fit to the Cer-N-γ_2 data was 22-fold greater than that for Cer-N-RGS7 (Fig. 6B). The ratios of CFP-C-β_5Cer-N-γ_2 intensity to Cer-N-γ_2 expression level and of CFP-C-β_5Cer-N-RGS7 intensity to Cer-N-RGS7 expression level were used to normalize the β_5-interacting abilities of γ_2 and RGS7 to their expression levels. As shown in Fig. 6C, these ratios were the same, indicating that γ_2 and RGS7 exhibit the same ability to interact with an excess of β_5 when tested one at a time. In contrast, minimal fluorescence intensity was obtained with CFP-C-β_1Cer-N-RGS7. When Cer-N-γ_2 and Cer-N-RGS7 were coexpressed with an excess of CFP-C-β_1, the intensity of CFP-C-β_1Cer-N-γ_2 was 254-fold greater than that of CFP-C-β_1Cer-N-RGS7 (Fig. 6D). Under these conditions, the expression level of Cer-N-γ_2 was 43-fold greater than that of Cer-N-RGS7 (Fig. 6E). The decreased expression of Cer-N-RGS7 relative to Cer-N-γ_2 when coexpressed with CFP-C-β_1 rather than CFP-C-β_5 suggests that, despite the Cer-N tag, the stability of Cer-N-RGS7 is at least partially dependent on interaction with β_5, consistent with losses of R7 family RGS proteins in β_5 knockout mice (Chen et al., 2003). In addition, the ratio of CFP-C-β_1Cer-N-γ_2 intensity to Cer-N-γ_2 expression level was 6-fold greater than

TABLE 1
Competition of CerN-γ subunits with YN-γ_2 for dimerization with CC-β_5 in live HEK-293 cells
Values represent the mean ± S.E. from three experiments.

γ subunit	IC_{50}[a]	CerN-γ Expression[b]	Normalized IC_{50}[c]
	μg of CerN-γ	*per μg (× 10⁻⁵)*	*× 10⁻⁵*
γ_1	3.10 ± 1.08	1.38 ± 0.23	4.27 ± 1.65
γ_2	0.15 ± 0.02	4.44 ± 0.77	0.66 ± 0.14
γ_5	2.15 ± 0.59	4.39 ± 0.17	9.43 ± 2.64
γ_7	0.40 ± 0.06	6.78 ± 0.58	2.68 ± 0.49
γ_{10}	2.66 ± 0.48	3.27 ± 0.07	8.71 ± 1.57
γ_{11}	1.94 ± 0.54	7.88 ± 0.58	15.27 ± 4.41
γ_{12}	1.60 ± 0.31	5.62 ± 0.46	9.01 ± 1.88

[a] Defined as micrograms of CerN-γ plasmid that produced a 50% decrease in the intensity of CC-β_5YN-γ_2, calculated from the data in Fig. 3D.
[b] Calculated from linear fits of CerN-γ expression per microgram plasmid. Expression levels were determined as described in the legend to Fig. 3E.
[c] Defined as IC_{50} × CerN-γ expression per microgram of plasmid.

that of CFP-C-β_1Cer-N-RGS7 intensity to Cer-N-RGS7 expression level (Fig. 6F).

β_5 Exhibited a Slight Preference for γ_2 over RGS7 That Was Eliminated in the Presence of R7BP. To determine whether preferential association of β_5 with γ_2 or RGS7 would be revealed when a limiting amount of β_5 was coexpressed with both γ_2 and RGS7 at the same time, we compared the abilities of Cer-N-RGS7 and Cer-N-γ_2 to compete with YFP-N-γ_2 for binding to CFP-C-β_5. The amount of yellow fluorescence obtained from CFP-C-β_5YFP-N-γ_2 was measured when a range of amounts of either Cer-N-RGS7 or Cer-N-γ_2 plasmid was coexpressed. The amount of Cer-N-RGS7 plasmid required to reduce the CFP-C-β_5YFP-N-γ_2 intensity by 50% was 8-fold higher than that of Cer-N-γ_2 (Fig. 7A). When the amounts of Cer-N-RGS7 and Cer-N-γ_2 plasmids used were normalized to their relative expression levels in the presence of limiting amounts of CFP-C-β_5, three times as much Cer-N-RGS7 compared with Cer-N-γ_2 was required to reduce the intensity of CFP-C-β_5YFP-N-γ_2 by 50% (Fig. 7B). Thus, $\beta_5\gamma_2$ and β_5RGS7 complexes can form simultaneously in intact cells, and β_5 exhibits a slight preference for γ_2 over RGS7 when coexpressed with both potential binding partners.

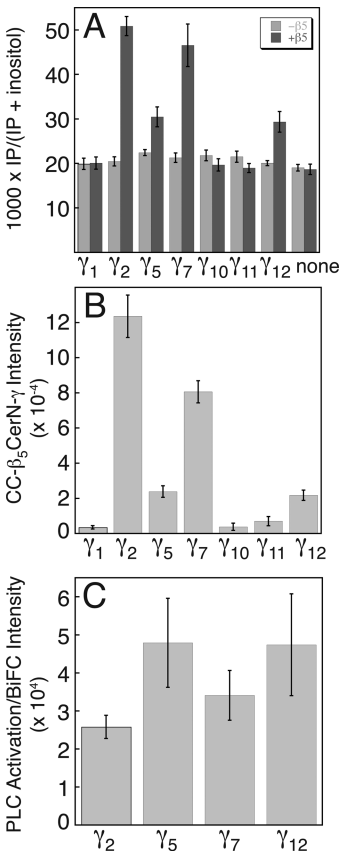

Fig. 4. Comparisons of the abilities of different β_5 and γ combinations to activate phospholipase C-β2 and to form complexes. A, activation of phospholipase C-β2 in cells expressing CFP-C-β_5 and Cer-N-γ subunits. HEK-293 cells were transfected with 3 μg of phospholipase C-β2 plasmid and, where indicated, 2.4 μg of CFP-C-β_5 plasmid and 0.3 μg of Cer-N-γ plasmids. The total amount of plasmid in each transfection was maintained at 5.7 μg by making up the difference with pcDNAI/Amp. Values represent the means ± S.E. from six experiments performed in triplicate. B, fluorescence intensities of CFP-C-β_5Cer-N-γ complexes expressed under the same transfection conditions as in A. Values represent the means ± S.E. from 3 experiments performed in duplicate. C, normalization of phospholipase C-β2 activation by coexpressed CFP-C-β_5 and Cer-N-γ subunits to the fluorescence intensities of the CFP-C-β_5Cer-N-γ complexes. Inositol phosphate levels obtained in cells transfected with pcDNAI/Amp (background) were subtracted from the levels in cells expressing CFP-C-β_5 and either Cer-N-γ_2, Cer-N-γ_5, Cer-N-γ_7, or Cer-N-γ_{12}. These background-subtracted activities were divided by the corresponding CFP-C-β_5Cer-N-γ intensities.

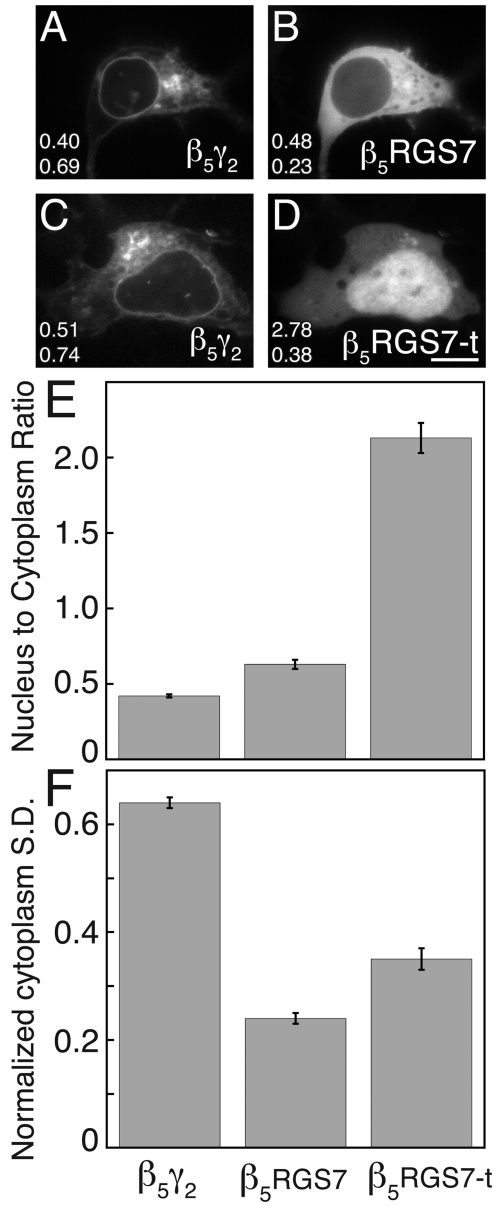

Fig. 5. Both γ_2 and RGS7 form complexes with β_5 that can be imaged simultaneously in the same cells using BiFC. YFP (A) and CFP (B) images from the same cell expressing CFP-C-β_5YFP-N-γ_2 and CFP-C-β_5Cer-N-RGS7. HEK-293 cells were transfected with the following quantities of plasmids: CFP-C-β_5, 0.3 μg; YFP-N-γ_2 and Cer-N-RGS7, 0.15 μg; and mCherry-Mem, 0.0025 μg. YFP (C) and CFP (D) images from the same cell expressing CFP-C-β_5YFP-N-γ_2 and CFP-C-β_5CFP-*N*-RGS7-t, which contains a truncated form of RGS7 lacking the DEP domain. HEK-293 cells were transfected with the following quantities of plasmids: CFP-C-β_5, 0.3 μg; YFP-N-γ_2 and CFP-*N*-RGS7-t, 0.15 μg; and mCherry-Mem, 0.0025 μg. The top numbers in the images are the ratios of average pixel intensity in the nucleus to that in the cytoplasm and the bottom numbers are the normalized cytoplasmic standard deviations of pixel intensity for the cells shown. E, ratios of average pixel intensity in the nucleus compared with the cytoplasm; F, normalized cytoplasmic standard deviations of pixel intensity for CFP-C-β_5YFP-N-γ_2, CFP-C-β_5Cer-N-RGS7, and CFP-C-β_5CFP-*N*-RGS7-t. Values represent the mean ± S.E. n = 113 for CFP-C-β_5YFP-N-γ_2, 64 for CFP-C-β_5Cer-N-RGS7, and 49 for CFP-C-β_5CFP-*N*-RGS7-t. Scale bar, 10 μm.

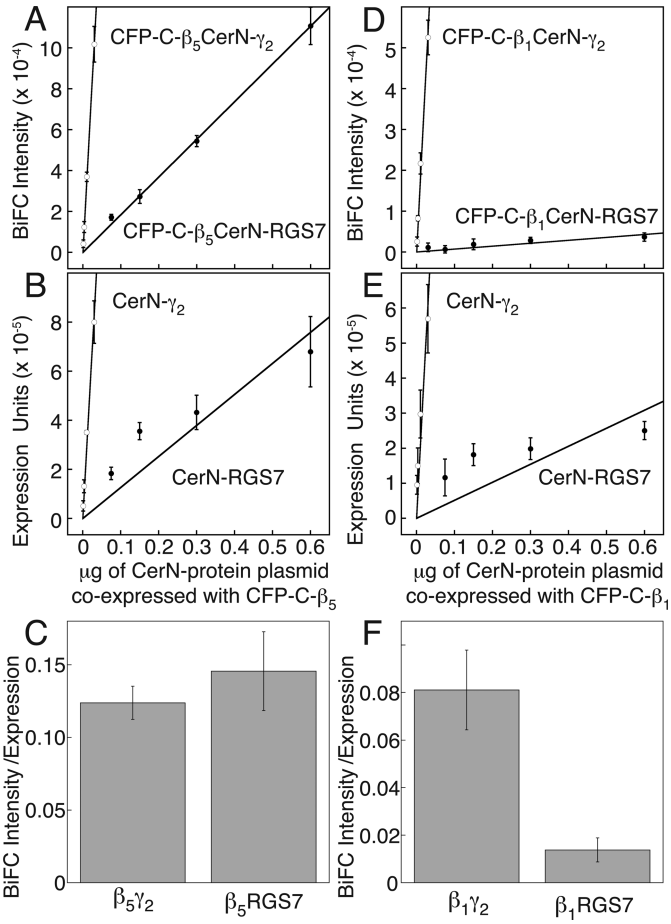

Fig. 6. Quantification of fluorescence and expression levels when Cer-N-γ_2 and Cer-N-RGS7 were coexpressed with an excess of either CFP-C-β_5 or CFP-C-β_1. A, intensities of CFP-C-β_5Cer-N-γ_2 and CFP-C-β_5Cer-N-RGS7 when CFP-C-β_5 is not limiting. HEK-293 cells were transfected with 2.4 μg of plasmid expressing CFP-C-β_5 and the indicated quantity of Cer-N-γ_2 or Cer-N-RGS7. The total amount of plasmid in each transfection was maintained at 3 μg using pcDNAI/Amp. Values represent the means ± S.E of three experiments performed in duplicate. From linear fits to the data, CFP-C-β_5Cer-N-γ_2 intensity per microgram of Cer-N-γ_2 plasmid ($\times 10^{-5}$) was 34.25 ± 2.89, and CFP-C-β_5Cer-N-RGS7 intensity per microgram of Cer-N-RGS7 plasmid ($\times 10^{-5}$) was 1.84 ± 0.14. B, expression levels of Cer-N-γ_2 and Cer-N-RGS7 when coexpressed with an excess of CFP-C-β_5. HEK-293 cells were transfected as in A. Values represent the means ± S.E from three experiments. From linear fits to the data, Cer-N-γ_2 expression per microgram of plasmid ($\times 10^{-6}$) was 27.67 ± 2.55, and Cer-N-RGS7 intensity per microgram of plasmid ($\times 10^{-6}$) was 1.26 ± 0.24. C, Normalization of CFP-C-β_5Cer-N-γ_2 and CFP-C-β_5Cer-N-RGS7 intensities to the expression levels of Cer-N-γ_2 and Cer-N-RGS7. The intensities per microgram of Cer-N-protein plasmid of CFP-C-β_5Cer-N-γ_2 and CFP-C-β_5Cer-N-RGS7 were divided by the expression per microgram of plasmid of Cer-N-γ_2 and Cer-N-RGS7, respectively. D, CFP-C-β_1 forms a fluorescent complex with Cer-N-γ_2 but not Cer-N-RGS7. HEK-293 cells were transfected as in A, except that CFP-C-β_1-expressing plasmid was substituted for CFP-C-β_5-expressing plasmid. Values represent the means ± S.E of three experiments performed in duplicate. From linear fits to the data, CFP-C-β_1Cer-N-γ_2 intensity per microgram of Cer-N-γ_2 plasmid ($\times 10^{-5}$) was 18.02 ± 1.52, and CFP-C-β_1Cer-N-RGS7 intensity per microgram of Cer-N-RGS7 plasmid ($\times 10^{-5}$) was 0.0714 ± 0.0233. E, expression levels of Cer-N-γ_2 and Cer-N-RGS7 when coexpressed with an excess of CFP-C-β_1. HEK-293 cells were transfected as in D. Values represent the means ± S.E from four experiments. From linear fits to the data, Cer-N-γ_2 expression per microgram of plasmid ($\times 10^{-6}$) was 22.22 ± 4.20, and Cer-N-RGS7 intensity per microgram of plasmid ($\times 10^{-6}$) was 0.52 ± 0.085. F, normalization of CFP-C-β_1Cer-N-γ_2 and CFP-C-β_1Cer-N-RGS7 intensities to the expression levels of Cer-N-γ_2 and Cer-N-RGS7. The intensities per microgram of Cer-N-protein plasmid of CFP-C-β_1Cer-N-γ_2 and CFP-C-β_1Cer-N-RGS7 were divided by the expression per microgram of plasmid of Cer-N-γ_2 and Cer-N-RGS7, respectively.

β_5RGS7 complexes can be targeted to the plasma membrane by R7BP, which, like β_5 and RGS7, is highly expressed in the nervous system (Drenan et al., 2006). To determine whether R7BP can influence the formation of $\beta_5\gamma_2$ and β_5RGS7 complexes, we investigated whether coexpression of R7BP, at levels which targeted β_5RGS7 to the plasma membrane (Fig. 7, C–E), affected competition between RGS7 and γ_2 for β_5. We found that coexpression of R7BP decreased the preference of β_5 for γ_2 over RGS7. In the presence of R7BP, the amount of Cer-N-RGS7 plasmid required to reduce the CFP-C-β_5YFP-N-γ_2 intensity by 50% was 5-fold higher than that of Cer-N-γ_2 (Fig. 7F). When the amounts of Cer-N-RGS7 and Cer-N-γ_2 plasmids used were normalized to their relative expression levels in the presence of R7BP and limiting amounts of CFP-C-β_5, approximately the same amounts of Cer-N-RGS7 and Cer-N-γ_2 reduced the intensity of CFP-C-β_5YFP-N-γ_2 by 50% (Fig. 7G).

γ_2 Exhibited a Preference for β_1 over β_5 When the Three Proteins Were Coexpressed. The above studies compared the preferences of β_5 for different interaction partners and demonstrated that γ_2 was preferred over the other six γ subunits tested and over RGS7 in the absence of R7BP. Because the prevalence of particular β_5 complexes will reflect the interaction preferences of both β_5 and its potential interaction partners, we investigated the interaction preferences of γ_2. The intensities of Cer-N-β_1CFP-C-γ_2 and Cer-N-β_5CFP-C-γ_2 complexes were compared as well as the abilities of Cer-N-β_1 and Cer-N-β_5 to compete with YFP-N-β_1 for interaction with CFP-C-γ_2.

In the presence of an excess of cotransfected CFP-C-γ_2 plasmid, linear relationships between the amounts of transfected Cer-N-β_1 and Cer-N-β_5 plasmids and the intensities of Cer-N-β_1CFP-C-γ_2 and Cer-N-β_5CFP-C-γ_2 complexes, respectively, were obtained, and the intensities of the complexes were similar (Fig. 8A). The relationships between the expression levels of Cer-N-β_1 and Cer-N-β_5 and the amounts of transfected plasmid under these expression conditions were also linear and similar (Fig. 8B), resulting in similar ratios of Cer-N-βCFP-C-γ_2 intensities to Cer-N-β subunit expression levels (Fig. 8C).

When the abilities of Cer-N-β_1 and Cer-N-β_5 to compete with YFP-N-β_1 for interaction with CFP-C-γ_2 were compared, the amount of Cer-N-β_5 plasmid required to reduce the YFP-N-β_1CFP-C-γ_2 intensity by 50% was 4.2-fold higher than of that of Cer-N-β_1 (Fig. 8D). The expression level of Cer-N-β_1 was 0.98-fold of that of Cer-N-β_5 in the presence of limiting amounts of CFP-C-γ_2 (S.E. = 0.10, n = 3). This preferential interaction of γ_2 with β_1 rather than β_5 might be expected to work against the preference of β_5 for γ_2 over RGS7 in cells coexpressing β_1, β_5, γ_2, and RGS7 by diverting some of the available γ_2 away from β_5.

$\beta_5\gamma_2$ and β_5RGS7 Were Targeted Preferentially to the Plasma Membrane by Inactive and Activated α_o, Respectively. Although $\beta_1\gamma_2$ and $\beta_2\gamma_2$ localize to the plasma membrane, $\beta_5\gamma_2$ accumulates on intracellular membranes, including the ER and the Golgi apparatus (Hynes et al., 2004b) (Figs. 1, 2, and 5). The ability of the β subunit to influence targeting of the γ subunit was surprising, because the β subunit is not known to have a membrane-targeting signal, such as the prenyl group on the γ subunit (Wedegaertner et al., 1995). Because α_o was reported recently to target β_5RGS7 to the plasma membrane (Takida et al., 2005), we

hypothesized that plasma membrane targeting of $\beta_5\gamma_2$ also might require α_o, which is not expressed in HEK-293 cells (Wang et al., 1999b). Indeed, we found that coexpressed α_o did target both Cer-C-β_5Cer-N-γ_2 and Cer-C-β_5Cer-N-RGS7 to the plasma membrane (Fig. 9, A–F). Because α subunits in the inactive rather than the activated state have a higher affinity for $\beta\gamma$ complexes, whereas RGS proteins interact preferentially with the activated form of α subunits, we investigated how targeting of $\beta_5\gamma_2$ and β_5RGS7 were affected by an α_o mutant, α_oR179C, that is constitutively activated as a result of decreased GTPase activity. In agreement with the expected preferences of $\beta_5\gamma_2$ and β_5RGS7, α_oR179C was less effective than α_o at targeting $\beta_5\gamma_2$ and more effective than α_o at targeting β_5RGS7 (Fig. 9, A–F). The expression levels of α_o and α_oR179C, determined by immunoblotting membrane preparations using an antibody to the EE epitope included in both constructs, were similar (Fig. 9G). These results suggest that the inactive form of α_o interacts preferentially with $\beta_5\gamma_2$, whereas activated α_o interacts preferentially with β_5RGS7.

α_o and α_q Exhibited Similar Abilities to Target $\beta_5\gamma_2$ to the Plasma Membrane. Our observation that α_o can target $\beta_5\gamma_2$ to the plasma membranes of live cells is consis-

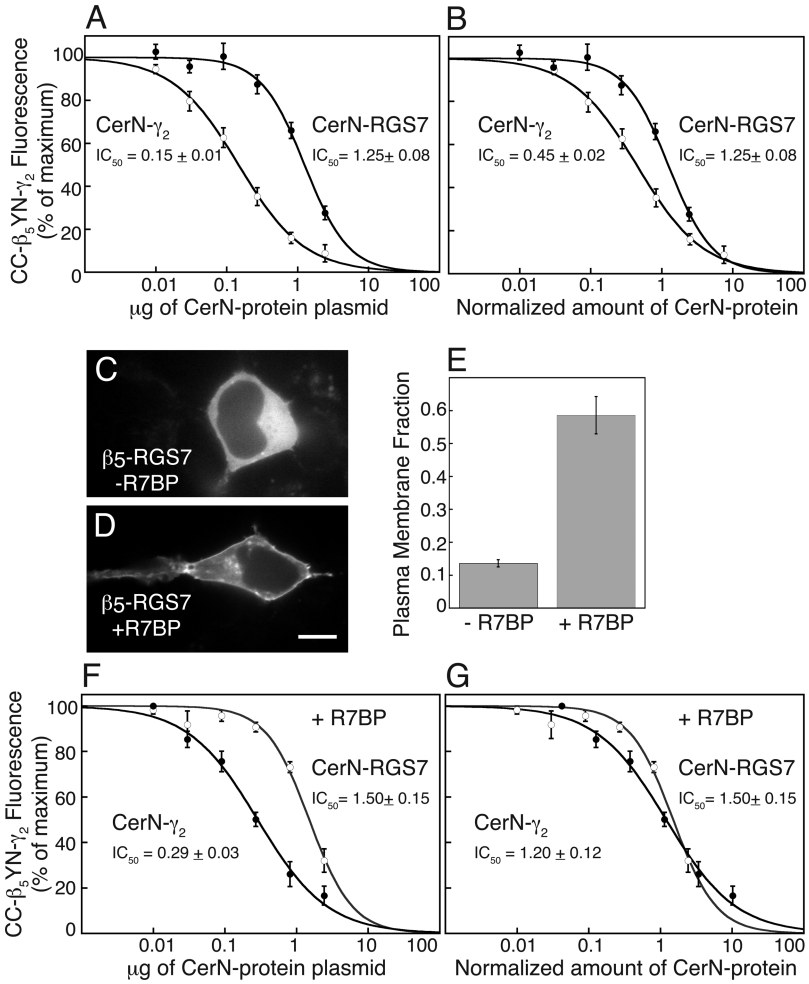

Fig. 7. Competition between γ_2 and RGS7 for limiting amounts of β_5. A and B, the intensity of CFP-C-β_5YFP-N-γ_2 was measured in the presence of Cer-N-γ_2, Cer-N-RGS7, or empty vector. 1.6×10^6 HEK-293 cells were transfected with 0.6 μg each of plasmids expressing CFP-C-β_5 and YFP-N-γ_2, and the indicated amount of Cer-N-γ_2 or Cer-N-RGS7. The total amount of plasmid in each transfection was maintained at 3.63 μg using pcDNAI/Amp. A, CFP-C-β_5YFP-N-γ_2 intensity expressed as a function of μg of cotransfected Cer-N-γ_2 or Cer-N-RGS7 plasmid. Values represent the means ± S.E. from seven experiments performed in duplicate. B, CFP-C-β_5YFP-N-γ_2 intensity expressed as a function of the relative amounts of coexpressed Cer-N-γ_2 or Cer-N-RGS7 plasmid. Expression levels were determined in 1.6×10^6 HEK-293 cells transfected with 0.6 μg each of plasmids expressing CFP-C-β_5 and pcDNAI/Amp, and 0.03, 0.09, 0.27, 0.81, or 2.43 μg of Cer-N-γ_2 or Cer-N-RGS7 plasmid. The total amount of plasmid in each transfection was maintained at 3.63 μg using pcDNAI/Amp. The expression level of Cer-N-γ_2 was 3.08-fold greater than that of Cer-N-RGS7 under these conditions (S.E. = 0.54, n = 4). Consequently, the plasmid amounts used for Cer-N-γ_2 expression in A were multiplied by this factor to normalize the expression levels of Cer-N-γ_2 and Cer-N-RGS7. C–E, R7BP targets CFP-C-β_5Cer-N-RGS7 to the plasma membrane. HEK-293 cells (2×10^5) were transfected with 0.075 μg of CFP-C-β_5 plasmid, 0.3038 μg of Cer-N-RGS7 plasmid, 0.0025 μg of mCherry-Mem plasmid, and, where indicated, 0.01875 μg of R7BP plasmid. Images of HEK-293 cells expressing CFP-C-β_5Cer-N-RGS7 in the absence (C) or presence (D) of R7BP. Scale bar, 10 μm. E, plasma membrane fraction of Cer-C-β_5Cer-N-RGS7 in the absence or presence of R7BP. Values represent the means ± S.E. n = 34 for CFP-C-β_5Cer-N-RGS7 in the absence of R7BP and 38 for CFP-C-β_5Cer-N-RGS7 in the presence of R7BP. F and G, in the presence of R7BP, CFP-C-β_5 exhibits similar preferences for Cer-N-γ_2 and Cer-N-RGS7. F, CFP-C-β_5YFP-N-γ_2 intensity is expressed as a function of the relative amounts of coexpressed Cer-N-γ_2 or Cer-N-RGS7. HEK-293 cells were transfected as in A except that 0.15 μg of R7BP plasmid was also transfected. G, CFP-C-β_5YFP-N-γ_2 intensity is expressed as a function of the relative amounts of coexpressed Cer-N-γ_2 or Cer-N-RGS7 plasmid. Values represent the means ± S.E of four experiments performed in duplicate. Expression levels were determined in HEK-293 cells transfected as in B except that 0.15 μg of R7BP plasmid was also transfected. The expression level of Cer-N-γ_2 was 4.20-fold greater than that of Cer-N-RGS7 under these conditions (S.E. = 0.59, n = 4). Consequently, the plasmid amounts used for Cer-N-γ_2 expression in F were multiplied by this factor to normalize the expression levels of Cer-N-γ_2 and Cer-N-RGS7. CC indicates CFP-C and YN indicates YFP-N.

tent with a previous in vitro study demonstrating that α_o can bind to $\beta_5\gamma_2$ and prevent activation of phospholipase C-β2 (Yoshikawa et al., 2000) but contrasts with two other studies in reconstituted systems suggesting that $\beta_5\gamma_2$ interacts with α_q but not other α subunits (Fletcher et al., 1998; Lindorfer et al., 1998). To investigate the α subunit specificity of $\beta_5\gamma_2$ in live cells, we compared the abilities of α_o and α_q to target $\beta_5\gamma_2$ to the plasma membrane using fluorescent versions of these α subunits in which YFP was inserted at the homologous location in each. This made it possible to compare Cer-C-β_5Cer-N-γ_2 targeting by equivalent amounts of plasma membrane-associated α_o-YFP and α_q-YFP. This was important because previously we found that a significant amount of α_q-GFP localized to the cytoplasm in addition to the plasma membrane (Hughes et al., 2001). Although Cer-C-β_5Cer-N-γ_2 expressed in the absence of an α-YFP subunit localized intracellularly (Fig. 10, A and B), both α_o-YFP (Fig. 10, C and D) and α_q-YFP (Fig. 10, E and F) targeted Cer-C-β_5Cer-N-γ_2 to the plasma membrane. When coexpressed with either α_o-YFP or α_q-YFP, the fraction of Cer-C-β_5Cer-N-γ_2 that associated with the plasma membrane varied linearly as a function of the ratio of α_o-YFP or α_q-YFP intensity in the plasma membrane to total cell intensity of Cer-C-β_5Cer-N-γ_2 (Fig. 10G). Moreover, the 2 α-YFP constructs exhibited the same efficacy at targeting Cer-C-β_5Cer-N-γ_2 to the plasma membrane.

Discussion

Using multicolor BiFC we have quantified the interaction preferences of the G protein β_5 subunit in intact cells, and found that β_5 exhibits a strong preference for γ_2 relative to six other γ subunits, and also exhibits a modest preference for γ_2 over RGS7. These results shed some light on the quandary that despite the ability of $\beta_5\gamma_2$ to modulate effectors (Watson et al., 1994; Zhang et al., 1996; Lindorfer et al., 1998; Zhou et al., 2000; Mirshahi et al., 2002; Lei et al., 2003), β_5 is only associated with R7 family RGS proteins (Witherow et al., 2000) when purified from tissues. The instability of $\beta_5\gamma_2$ dimers under nondenaturing buffer conditions (Jones and Garrison, 1999; Jones et al., 2004) may explain why they have not been isolated and illustrates the advantage of using BiFC in intact cells to identify protein interaction partners. The ability of $\beta_5\gamma_2$ to be targeted to the plasma membrane by α subunits supports the conclusion that functional $\beta_5\gamma_2$ complexes can form in intact cells and mediate signaling by G

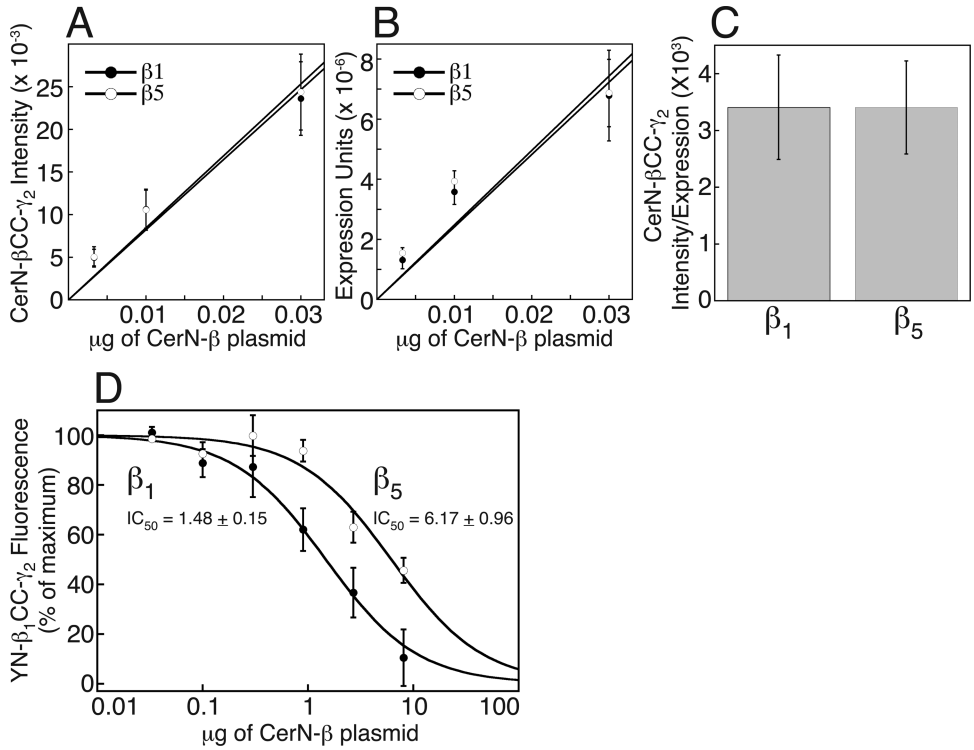

Fig. 8. β_1 competes more effectively than β_5 for limiting amounts of γ_2. A, intensities of Cer-N-β_1CFP-C-γ_2 and Cer-N-β_5CFP-C-γ_2 when CFP-C-γ_2 is not limiting. HEK-293 cells were transfected with 2.4 μg of plasmid expressing CFP-C-γ_2 and the indicated μg of plasmid expressing Cer-N-β_1 or Cer-N-β_5. The total amount of plasmid in each transfection was maintained at 2.43 μg using pcDNAI/Amp. Values represent the means ± S.E of four experiments performed in duplicate. Cer-N-β-CFP-C-γ_2 intensities per microgram of Cer-N-β plasmid, determined from linear fits to the data, were as follows (means ± S.E, × 10^{-5}): $\beta_1\gamma_2$, 8.22 ± 1.53; $\beta_5\gamma_2$, 8.44 ± 1.59. B, expression levels of Cer-N-β_1 and Cer-N-β_5 when coexpressed with excess CFP-C-γ_2. HEK-293 cells were transfected as in A. Values represent the means ± S.E from three experiments. Cer-N-β expression per microgram of plasmid, determined from linear fits to the data, were as follows (means ± S.E, × 10^{-8}): β_1, 2.41 ± 0.47; β_5, 2.48 ± 0.37. C, normalization of Cer-N-βCFP-C-γ_2 intensities to Cer-N-β expression levels. The intensity per microgram of Cer-N-β plasmid of each Cer-N-βCFP-C-γ_2 complex was divided by the corresponding Cer-N-β expression per microgram of plasmid. D, competition between Cer-N-β_1 or Cer-N-β_5 and YFP-N-β_1 for limiting amounts of CFP-C-γ_2. The intensity of YFP-N-β_1CFP-C-γ_2 was measured in the presence of Cer-N-β_1, Cer-N-β_5, or empty vector. HEK-293 cells were transfected with 0.3 μg of CFP-C-γ_2-expressing plasmid, 0.6 μg of YFP-N-β_1-expressing plasmid, and the indicated μg of either Cer-N-β_1 or Cer-N-β_5 plasmid. The total amount of plasmid in each transfection was maintained at 9 μg using pcDNAI/Amp. Values represent the means ± S.E. from five experiments performed in duplicate. Expression levels were determined in HEK-293 cells transfected with 0.3 μg of CFP-C-γ_2-expressing plasmid, 0.6 μg of pcDNAI/Amp, and the same range of micrograms of Cer-N-β_1 or Cer-N-β_5 plasmid, maintaining the total amount of plasmid in each transfection at 9 μg using pcDNAI/Amp. CC, CFP-C; YN, YFP-N.

protein-coupled receptors. The relative amounts of $\beta_5\gamma$ versus β_5R7 complexes in vivo will be influenced by the expression levels of potential β_5 binding partners in addition to the association preferences of β_5. Moreover, in the presence of coexpressed R7BP, β_5 exhibited similar preferences for γ_2 and RGS7. Furthermore, γ_2 interacted preferentially with β_1 rather than β_5. Taken together, these results suggest that multiple coexpressed proteins affect β_5 complex formation.

The interaction preferences of β_5 identified using BiFC probably reflect association preferences, because BiFC generally seems to be irreversible (Kerppola, 2006). Efforts are under way in a number of laboratories to develop a reversible form of BiFC, which would enable dynamic analysis of reversible protein-protein interactions. Nevertheless, because monomeric β subunits and R7 family proteins are degraded rapidly in living cells (Wang et al., 1999a; Witherow et al., 2000; Chen et al., 2003), it seems unlikely that β_5 exchanges binding partners in vivo. Association preferences identified using BiFC may reflect protein affinities, but other factors, such as accessibility or association with endogenous proteins, could also regulate complex formation in vivo. Comparisons of the affinities of β_5 for different γ subunits may be possible in vitro, because purified β_5 and γ_2 can be separated and then reassembled as a functional complex (Yoshikawa et al., 2000). However, it is not clear that RGS7 folds properly when expressed alone (Posner et al., 1999) or can be dissociated from β_5 in a functional form. Alternatively, an elegant means of corroborating BiFC results is a recently described proximity ligation in situ assay that enables visualization of endogenous protein complexes in fixed samples (Söderberg et al., 2006).

Competition between R7 family RGS proteins and γ subunits for association with β_5 and between β_1 and β_5 for γ_2 is likely to be of functional significance. Coexpression of RGS6 or RGS11 with β_5 and γ_2 was found previously to impair $\beta_5\gamma_2$-mediated inhibition of N-type Ca^{+2} channels (Zhou et al., 2000). In addition, GIRK channels are activated by $\beta\gamma$ complexes containing β_{1-4} and inhibited by $\beta_5\gamma$ complexes (Mirshahi et al., 2002; Lei et al., 2003). Our results suggest that β_5 can inhibit GIRK channels both by means of competition between $\beta_5\gamma$ and other $\beta\gamma$ complexes for GIRK channel binding and via competition between β_5 and other β subunits for γ subunit interaction.

Our observation that amounts of $\beta_5\gamma$ complex formation correlated with efficacies of phospholipase C-β2 activation suggests that previous observations of the greater functionality of $\beta_5\gamma_2$ compared with other $\beta_5\gamma$ complexes (Watson et al., 1994, 1996; Zhou et al., 2000) resulted from more efficient formation of $\beta_5\gamma_2$ dimers compared with the other combinations. Comparisons of the BiFC intensities and activities of $\beta\gamma$ complexes should be a widely applicable means of elucidating the functional importance of specific $\beta\gamma$ combinations in living cells.

The range of interaction preferences of β_5 for the seven γ subunits studied was greater than that of β_1 (Mervine et al., 2006). There were also differences in the relative order of

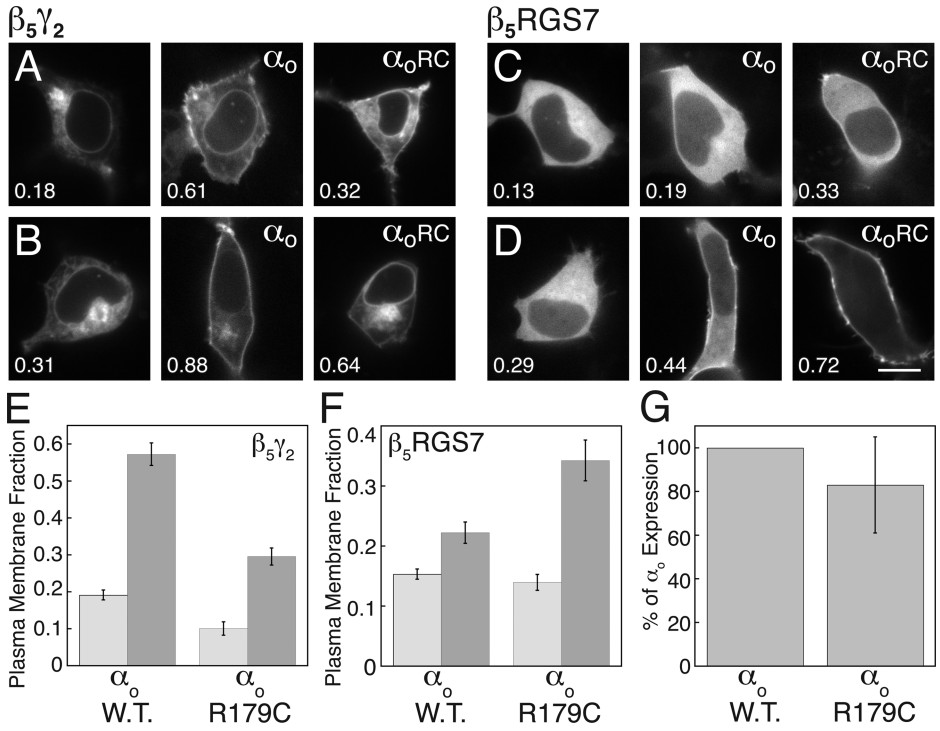

Fig. 9. Plasma membrane targeting of $\beta_5\gamma_2$ and β_5RGS7 by wild-type and constitutively activated α_o. HEK-293 cells were transfected with 0.075 μg of Cer-C-β_5 plasmid and 0.0025 μg of mCherry-Mem plasmid and either 0.075 μg of Cer-N-γ_2 plasmid (A and B) or 0.15 μg of Cer-N-RGS7 plasmid (C and D) in the absence or presence of 0.2 μg of plasmid encoding α_o or α_oR179C, as indicated. The plasma membrane fractions of Cer-C-β_5Cer-N-γ_2 and Cer-C-β_5Cer-N-RGS7 for the cells shown are indicated on the images. A, images of cells expressing Cer-C-β_5Cer-N-γ_2 with plasma membrane fractions similar to the mean values in E. B, images of cells expressing Cer-C-β_5Cer-N-γ_2 with plasma membrane fractions in the 85th to 95th percentile of all values. C, images of cells expressing Cer-C-β_5Cer-N-RGS7 with plasma membrane fractions similar to the mean values in F. D, images of cells expressing Cer-C-β_5Cer-N-RGS7 with plasma membrane fractions in the 85th to 95th percentile of all values. Scale bar, 10 μm. E and F, plasma membrane fractions of Cer-C-β_5Cer-N-γ_2 (E) and Cer-C-β_5Cer-N-RGS7 (F) in the absence (light gray bars) or presence (dark gray bars) of α_o or α_oR179C. Values represent the means ± S.E. from 64–128 cells. G, comparison of the expression levels of α_o and α_oR179C. Values represent the means ± S.E from three experiments.

effectiveness of the γ subunits in competing for β_5 versus β_1. In the case of β_1, γ_{12} was the most effective competitor, followed by γ_2 and γ_7, whereas γ_1 was the weakest. In contrast, γ_2 was the most effective competitor for β_5, followed by γ_7 and γ_1, whereas γ_{12} was one of the weaker competitors. In a given cell, the $\beta\gamma$ complexes that predominate will reflect both the interaction preferences and expression levels of each expressed β and γ subunit.

Our imaging results indicate that the interaction partner of β_5 plays an important role in the targeting of β_5 complexes. Some complexes containing β_5 ($\beta_5\gamma_1$, $\beta_5\gamma_5$, $\beta_5\gamma_{10}$, and $\beta_5\gamma_{11}$) exhibited significant localization to the nucleus in addition to the cytoplasm, whereas others ($\beta_5\gamma_2$, $\beta_5\gamma_7$, $\beta_5\gamma_{12}$, and β_5RGS7) localized predominantly to the cytoplasm. There is evidence for transcriptional regulation by RGS proteins (Burchett, 2003), but the potential functions of $\beta_5\gamma$ complexes in the nucleus remain to be elucidated. The type of signal exhibited by cytoplasmic β_5 complexes was also determined by the interacting partner, ranging from being diffuse (γ_1 and RGS7) to discrete (γ_2, γ_5, γ_7, γ_{10}, γ_{11}, γ_{12}).

β_5 also influences the localization of $\beta_5\gamma$ complexes, because complexes containing β_1 and each of the seven γ subunits studied here localized to the plasma membrane (Mervine et al., 2006). β Subunits, unlike prenylated γ subunits, lack an identified membrane-targeting signal (Wedegaertner et al., 1995). Instead, the membrane-targeting signal of β_5 seems to be α subunit interaction, because coexpression with an α subunit targeted both $\beta_5\gamma_2$ and β_5RGS7 to the plasma membrane. A significant amount of $\beta_5\gamma_2$ colocalized with either the ER or the Golgi apparatus, suggesting that interaction with α subunits can occur at these locations, resulting in plasma membrane targeting. Similar results and conclusions were reported previously for $\beta_1\gamma$ complexes (Michaelson et al., 2002; Takida and Wedegaertner, 2003), whereas we observed relatively minor effects of α subunits on $\beta_1\gamma$ targeting (Mervine et al., 2006). Differences in the observed dependence of heterologously expressed $\beta_1\gamma$ complexes on coexpressed α subunits for plasma membrane targeting are most likely due to differences in the expression levels of the transfected $\beta_1\gamma$ complexes relative to endogenous α subunits.

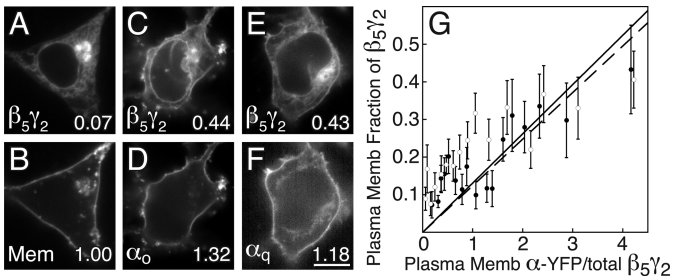

Fig. 10. α_o-YFP and α_q-YFP exhibit equivalent abilities to target Cer-C-β_5Cer-N-γ_2 to the plasma membrane. HEK-293 cells were transfected with 0.075 μg each of Cer-C-β_5 and Cer-N-γ_2 plasmids, and 0.0025 μg of mCherry-Mem plasmid, and either 0, 0.0125, 0.025, 0.05, or 0.075 μg of α_o-YFP plasmid or 0.025, 0.05, or 0.1 μg of α_q-YFP plasmid. A and B, image of cell coexpressing Cer-C-β_5Cer-N-γ_2 (A) and mCherry-Mem (B). C and D, image of cell coexpressing Cer-C-β_5Cer-N-γ_2 (C) and α_o-YFP (D). E and F, image of cell coexpressing Cer-C-β_5Cer-N-γ_2 (E) and α_q-YFP (F). The plasma membrane fractions of the fluorescent proteins are indicated on the images. G, plot of plasma membrane fraction of Cer-C-β_5Cer-N-γ_2 as a function of the ratio of the average plasma membrane intensity of α_o-YFP (open circles, solid line) or α_q-YFP (filled circles, dashed line) to the average cellular intensity of Cer-C-β_5Cer-N-γ_2. Measurements from individual cells were sorted into bins of 10 cells along the x-axis and averaged. Values represent the means ± S.E. 160 cells coexpressing Cer-C-β_5Cer-N-γ_2 and α_o-YFP and 170 cells coexpressing Cer-C-β_5Cer-N-γ_2 and α_q-YFP were analyzed.

Our targeting assay results address the issue of which α subunit(s) $\beta_5\gamma_2$ interacts with. $\beta_5\gamma_2$ was targeted to the plasma membrane by α_o and α_q to the same extent. Two previous studies suggested that $\beta_5\gamma_2$ interacts with α_q, but not other α subunits, including α_o. For instance, $\beta_5\gamma_2$ coupled the M1 muscarinic and ETB receptors to G_q, but failed to couple the ETB receptor to G_{i1} in a reconstituted system (Lindorfer et al., 1998). In another study using purified proteins or membrane extracts, $\beta_5\gamma_2$ interacted exclusively with α_q and not α_{i1}, α_{i2}, α_o, or α_s (Fletcher et al., 1998). However, a third study demonstrated that α_o could bind to $\beta_5\gamma_2$ and prevent activation of phospholipase C-β2 (Yoshikawa et al., 2000). The lack of plasma membrane targeting of $\beta_5\gamma_2$ in the absence of a coexpressed α subunit suggests that the endogenous α_q expressed in HEK-293 cells is insufficient for targeting heterologously expressed $\beta_5\gamma_2$, just as endogenous $\beta\gamma$ is unable to target overexpressed α_s (Mervine et al., 2006) (Fig. 1H).

Subcellular localization of β_5R7 complexes seems to be regulated by many factors. α_o-mediated targeting of β_5RGS7 involves α_o-promoted palmitoylation of RGS7 (Takida et al., 2005). The preferential interaction between β_5RGS7 and active rather than inactive α_o (Takida et al., 2005) (Fig. 9) suggests plasma membrane localization of β_5R7 complexes could be induced upon G protein activation. Subcellular localization of β_5RGS7 is also regulated by association with R7BP (Drenan et al., 2006) and may also be influenced by interaction with 14-3-3 proteins (Benzing et al., 2002). In addition, the DEP domains of certain RGS proteins can target them to specific G protein-coupled receptors (Kovoor et al., 2005; Ballon et al., 2006). Relationships between this multitude of factors that potentially can regulate β_5R7 localization and function remain to be elucidated.

Taken together with previously reported findings, our data are consistent with a model in which $\beta_5\gamma_2$ and β_5RGS7 interact preferentially with the inactive and activated forms of α_o, respectively. When α_o was reconstituted into phospholipid vesicles with $\beta_1\gamma_2$ and the M2 muscarinic receptor, β_5RGS7 activated the GTPase activity of α_o upon carbachol stimulation (Hooks et al., 2003). A plausible scenario is that $\beta_5\gamma_2$, like other $\beta\gamma$ complexes, associates with inactive α subunits and plays a role in mediating specific interactions with G protein-coupled receptors. In this scheme, receptor-mediated activation of $\alpha\beta_5\gamma_2$ complexes leads to modulation of effectors such as phospholipase C-β_2, GIRK channels, and N-type Ca^{+2} channels, whereas activation of $\alpha_o\beta\gamma$ complexes enables β_5RGS7 to bind to and activate the GTPase activity of α_o to regulate the kinetics of effector modulation by G_o. In addition, because some RGS proteins can interact directly with receptors (Kovoor et al., 2005; Ballon et al., 2006), the signaling pathways of certain receptors may be mediated entirely by $\alpha_o\beta_5$RGS7 complexes without the involvement of $\beta\gamma$ dimers.

Acknowledgments

We thank David Piston (Vanderbilt University, Nashville, TN) for the monomeric cerulean plasmid, Roger Tsien (University of California, San Diego, CA) for the mCherry plasmid, Janet Robishaw (Geisinger Clinic, Danville, PA) for plasmids expressing β and γ subunits, Kendall Blumer (Washington University, St. Louis, MO) for

the 3FLAG-R7BP plasmid, and Ravi Iyengar (Mount Sinai School of Medicine, New York, NY) for the human phospholipase C-β2 plasmid.

References

Ballon DR, Flanary PL, Gladue DP, Konopka JB, Dohlman HG, and Thorner J (2006) DEP-domain-mediated regulation of GPCR signaling responses. *Cell* **126:** 1079–1093.

Benzing T, Kottgen M, Johnson M, Schermer B, Zentgraf H, Walz G, and Kim E (2002) Interaction of 14-3-3 protein with regulator of G protein signaling 7 is dynamically regulated by tumor necrosis factor-α. *J Biol Chem* **277:**32954–32962.

Burchett SA (2003) In through the out door: nuclear localization of the regulators of G protein signaling. *J Neurochem* **87:**551–559.

Chatterjee TK, Liu Z, and Fisher RA (2003) Human RGS6 gene structure, complex alternative splicing, and role of N terminus and G protein γ-subunit-like (GGL) domain in subcellular localization of RGS6 splice variants. *J Biol Chem* **278:** 30261–30271.

Chen CK, Eversole-Cire P, Zhang H, Mancino V, Chen YJ, He W, Wensel TG, and Simon MI (2003) Instability of GGL domain-containing RGS proteins in mice lacking the G protein β-subunit Gβ_5. *Proc Natl Acad Sci U S A* **100:**6604–6609.

Drenan RM, Doupnik CA, Jayaraman M, Buchwalter AL, Kaltenbronn KM, Huettner JE, Linder ME, and Blumer KJ (2006) R7BP augments the function of RGS7-Gβ_5 complexes by a plasma membrane-targeting mechanism. *J Biol Chem* **281:** 28222–28231.

Fletcher JE, Lindorfer MA, DeFilippo JM, Yasuda H, Guilmard M, and Garrison JC (1998) The G protein β_5 subunit interacts selectively with the $G_q\alpha$ subunit. *J Biol Chem* **273:**636–644.

Grinberg AV, Hu CD, and Kerppola TK (2004) Visualization of Myc/Max/Mad family dimers and the competition for dimerization in living cells. *Mol Cell Biol* **24:**4294–4308.

Hooks SB, Waldo GL, Corbitt J, Bodor ET, Krumins AM, and Harden TK (2003) RGS6, RGS7, RGS9, and RGS11 stimulate GTPase activity of G_i family G-proteins with differential selectivity and maximal activity. *J Biol Chem* **278:**10087–10093.

Hughes TE, Zhang H, Logothetis DE, and Berlot CH (2001) Visualization of a functional Gα_q-green fluorescent protein fusion in living cells. Association with the plasma membrane is disrupted by mutational activation and by elimination of palmitoylation sites, but not by activation mediated by receptors or AlF_4^-. *J Biol Chem* **276:**4227–4235.

Hynes TR, Mervine SM, Yost EA, Sabo JL, and Berlot CH (2004a) Live cell imaging of G_s and the β_2-adrenergic receptor demonstrates that both α_s and $\beta_1\gamma_7$ internalize upon stimulation and exhibit similar trafficking patterns that differ from that of the β_2-adrenergic receptor. *J Biol Chem* **279:**44101–44112.

Hynes TR, Tang L, Mervine SM, Sabo JL, Yost EA, Devreotes PN, and Berlot CH (2004b) Visualization of G protein $\beta\gamma$ dimers using bimolecular fluorescence complementation demonstrates roles for both β and γ in subcellular targeting. *J Biol Chem* **279:**30279–30286.

Jones MB and Garrison JC (1999) Instability of the G-protein β_5 subunit in detergent. *Anal Biochem* **268:**126–133.

Jones MB, Siderovski DP, and Hooks SB (2004) The G $\beta\gamma$ dimer as a novel source of selectivity in G-protein signaling: GGL-ing at convention. *Mol Interv* **4:**200–214.

Kerppola TK (2006) Visualization of molecular interactions by fluorescence complementation. *Nat Rev Mol Cell Biol* **7:**449–456.

Kovoor A, Chen CK, He W, Wensel TG, Simon MI, and Lester HA (2000) Coexpression of Gβ_5 enhances the function of two Gγ subunit-like domain-containing regulators of G protein signaling proteins. *J Biol Chem* **275:**3397–3402.

Kovoor A, Seyffarth P, Ebert J, Barghshoon S, Chen CK, Schwarz S, Axelrod JD, Cheyette BN, Simon MI, Lester HA, et al. (2005) D2 dopamine receptors colocalize regulator of G-protein signaling 9–2 (RGS9–2) via the RGS9 DEP domain, and RGS9 knock-out mice develop dyskinesias associated with dopamine pathways. *J Neurosci* **25:**2157–2165.

Lei Q, Jones MB, Talley EM, Garrison JC, and Bayliss DA (2003) Molecular mechanisms mediating inhibition of G protein-coupled inwardly-rectifying K^+ channels. *Mol Cells* **15:**1–9.

Lindorfer MA, Myung CS, Savino Y, Yasuda H, Khazan R, and Garrison JC (1998) Differential activity of the G protein $\beta_5\gamma$2 subunit at receptors and effectors. *J Biol Chem* **273:**34429–34436.

Medina R, Grishina G, Meloni EG, Muth TR, and Berlot CH (1996) Localization of the effector-specifying regions of $G_{i2\alpha}$ and $G_{q\alpha}$. *J Biol Chem* **271:**24720–24727.

Mervine SM, Yost EA, Sabo JL, Hynes TR, and Berlot CH (2006) Analysis of G Protein $\beta\gamma$ dimer formation in live cells using multicolor bimolecular fluorescence complementation demonstrates preferences of β_1 for particular gamma subunits. *Mol Pharmacol* **70:**194–205.

Michaelson D, Ahearn I, Bergo M, Young S, and Philips M (2002) Membrane trafficking of heterotrimeric G proteins via the endoplasmic reticulum and Golgi. *Mol Biol Cell* **13:**3294–3302.

Mirshahi T, Robillard L, Zhang H, Hebert TE, and Logothetis DE (2002) Gβ residues that do not interact with Gα underlie agonist-independent activity of K^+ channels. *J Biol Chem* **277:**7348–7355.

Posner BA, Gilman AG, and Harris BA (1999) Regulators of G protein signaling 6 and 7. Purification of complexes with Gβ_5 and assessment of their effects on G protein-mediated signaling pathways. *J Biol Chem* **274:**31087–31093.

Rizzo MA, Springer GH, Granada B, and Piston DW (2004) An improved cyan fluorescent protein variant useful for FRET. *Nat Biotechnol* **22:**445–449.

Shaner NC, Campbell RE, Steinbach PA, Giepmans BN, Palmer AE, and Tsien RY (2004) Improved monomeric red, orange and yellow fluorescent proteins derived from Discosoma sp. red fluorescent protein. *Nat Biotechnol* **22:**1567–1572.

Snow BE, Krumins AM, Brothers GM, Lee SF, Wall MA, Chung S, Mangion J, Arya S, Gilman AG, and Siderovski DP (1998) A G protein γ subunit-like domain shared between RGS11 and other RGS proteins specifies binding to Gβ_5 subunits. *Proc Natl Acad Sci U S A* **95:**13307–13312.

Söderberg O, Gullberg M, Jarvius M, Ridderstrale K, Leuchowius KJ, Jarvius J, Wester K, Hydbring P, Bahram F, Larsson LG, et al. (2006) Direct observation of individual endogenous protein complexes in situ by proximity ligation. *Nat Methods* **3:**995–1000.

Takida S, Fischer CC, and Wedegaertner PB (2005) Palmitoylation and plasma membrane targeting of RGS7 are promoted by α_o. *Mol Pharmacol* **67:**132–139.

Takida S and Wedegaertner PB (2003) Heterotrimer formation, together with isoprenylation, is required for plasma membrane targeting of G$\beta\gamma$. *J Biol Chem* **278:**17284–17290.

Wang Q, Mullah B, Hansen C, Asundi J, and Robishaw JD (1997) Ribozyme-mediated suppression of the G protein γ_7 subunit suggests a role in hormone regulation of adenylylcyclase activity. *J Biol Chem* **272:**26040–26048.

Wang Q, Mullah BK, and Robishaw JD (1999a) Ribozyme approach identifies a functional association between the G protein $\beta_1\gamma_7$ subunits in the β-adrenergic receptor signaling pathway. *J Biol Chem* **274:**17365–17371.

Wang Y, Windh RT, Chen CA and Manning DR (1999b) *N*-Myristoylation and $\beta\gamma$ play roles beyond anchorage in the palmitoylation of the G protein α_o subunit. *J Biol Chem* **274:**37435–37442.

Watson AJ, Aragay AM, Slepak VZ, and Simon MI (1996) A novel form of the G protein β subunit Gβ_5 is specifically expressed in the vertebrate retina. *J Biol Chem* **271:**28154–28160.

Watson AJ, Katz A, and Simon MI (1994) A fifth member of the mammalian G-protein β-subunit family. Expression in brain and activation of the β2 isotype of phospholipase C. *J Biol Chem* **269:**22150–22156.

Wedegaertner PB, Wilson PT, and Bourne HR (1995) Lipid modifications of trimeric G proteins. *J Biol Chem* **270:**503–506.

Witherow DS, Wang Q, Levay K, Cabrera JL, Chen J, Willars GB, and Slepak VZ (2000) Complexes of the G protein subunit Gβ_5 with the regulators of G protein signaling RGS7 and RGS9. Characterization in native tissues and in transfected cells. *J Biol Chem* **275:**24872–24880.

Yoshikawa DM, Hatwar M, and Smrcka AV (2000) G protein β_5 subunit interactions with alpha subunits and effectors. *Biochemistry* **39:**11340–11347.

Zhang S, Coso OA, Lee C, Gutkind JS, and Simonds WF (1996) Selective activation of effector pathways by brain-specific G protein β_5. *J Biol Chem* **271:**33575–33579.

Zhou JY, Siderovski DP, and Miller RJ (2000) Selective regulation of N-type Ca channels by different combinations of G-protein $\beta\gamma$ subunits and RGS proteins. *J Neurosci* **20:**7143–7148.

Address correspondence to: Catherine Berlot, Weis Center for Research, Geisinger Clinic, 100 North Academy Avenue, Danville, PA 17822-2623. E-mail: chberlot@geisinger.edu